

1 **Sedimentology and the facies architecture of the Ghaggar-Hakra Formation, Barmer Basin,**

2 **India: Implications for early Cretaceous deposition on the north-western Indian Plate**

3 **margin**

4 Hazel Beaumont^{1*}, Stuart M. Clarke¹, Stuart D. Burley^{1&2}, Andrew M. Taylor³, and Pinak
5 Mohapatra⁴

6 ¹Basin Dynamics Research Group, School of Geography, Geology and the Environment, Keele University,
7 Staffordshire, UK

8 ²Orient Petroleum Limited, PTET House, Mauve Area, G-10/4, Islamabad, Pakistan

9 ³Skolithos Ltd., The White House, Higher Banks, Mellor, Lancashire, UK

10 ⁴Cairn India Ltd., DLF Atria, Jacaranda Marg, Gurgaon, India

11

12 *Current address: Department of Geography and Environmental Management, University of the West of
13 England Bristol, Bristol, UK

14 hazel.beaumont@uwe.ac.uk

15

16 **ABSTRACT**

17 Fluvial strata of the Lower Cretaceous Ghaggar-Hakra Formation are exposed in fault blocks
18 on the central-eastern margin of the Barmer Basin, Rajasthan. The sedimentology of these
19 outcrops is described from 114 logs (thicknesses up to 100 m) and 53 two-dimensional
20 correlation panels. The formation comprises three distinct channel-belt sandstone packages
21 defined as the Darjaniyon-ki Dhani, Sarnoo and Nosar sandstones separated by thick
22 siltstone-dominated floodplain successions. The sediments were deposited in a sub-tropical,
23 low sinuosity fluvial system that matures into a highly sinuous fluvial system. The Nosar
24 Sandstone, the youngest of the three packages, exhibits a significant increase in energy and
25 erosive power compared to those underlying it. This distinct change in fluvial style is
26 interpreted to be rejuvenation due to an actively developing rift network forming
27 accommodation space, rather than climatic controls acting on part of the depositional
28 system. Consequently, the Ghaggar-Hakra Formation at outcrop represents Lower
29 Cretaceous syn-rift deposition within the Barmer Basin with active localised fault movement

30 from Nosar Sandstone times onward. These findings provide sedimentological evidence in
31 support of pre-Palaeogene northwest-southeast extension in the Barmer Basin. Moreover,
32 they imply Cretaceous extension took place widely along the northern extremity of the West
33 Indian Rift System consistent with plate tectonic models of the break-up of Gondwana and
34 evolution of the Indian Ocean. Outcrops of Lower Cretaceous strata are patchy across India
35 and Pakistan. This study provides valuable material which, when combined with the
36 available published data, facilitates a re-evaluation of Lower Cretaceous palaeogeography
37 for the northwest Indian Plate. The reconstruction demonstrates a complex fluvial system,
38 where the sediments are preserved sporadically as early syn-rift strata. The findings imply a
39 high preservation potential for early Cretaceous fluvial successions within rifted fault blocks
40 near Saraswati and Ashiwarya of the Barmer Basin beneath the Palaeogene fill that likely
41 have significant potential for further hydrocarbon exploration.

42 **Key words:** Barmer Basin, fluvial, Ghaggar-Hakra Formation, palaeogeography, tectonics.

43

44

45

46

47

48

49

50

51

52 **Introduction**

53 The Barmer Basin is the northern most basin of a series of rifts that comprise the West
54 Indian Rift System (WIRS; Fig. 1A), and hosts large hydrocarbon reserves within continental
55 sediments of the basin fill (Dolson *et al.*, 2015). However, the early geological history of the
56 basin, and the nature of the Mesozoic sedimentary fill, remain poorly understood. This lack
57 of knowledge stems mostly from the limited surface exposure which restricts outcrop
58 studies and thereby constrains interpretations of subsurface well and seismic data.

59 The Barmer Basin was considered to have developed in response to passage of the Indian
60 Plate over the Reunion hotspot, giving rise to a syn- and post-rift Palaeogene to Eocene
61 sedimentary fill, overlying Precambrian rocks of the Malani Igneous Suite (Fig. 2A, Crawford
62 & Compton, 1969) and pre-rift Mesozoic sediments (Sisodia & Singh, 2000; Compton, 2009).
63 Recently, an important earlier northwest – southeast extensional event has been recognised,
64 preserved in structural geometries exposed on the basin margins and overprinted by the
65 perceived main Palaeogene rifting (Bladon *et al.*, 2015b; Dasgupta & Mukerjee, 2017). Fluvial
66 sediments preserved on the rift margin are ascribed to the Lower Cretaceous Ghaggar-Hakra
67 Formation and rift-margin geometries suggest that they were deposited contemporaneously
68 with the pre-Palaeogene normal faulting (Bladon *et al.*, 2015a, b). Although the Ghaggar-
69 Hakra Formation occurs in relatively small outcrops around Sarnoo, they are regionally
70 significant as they provide excellent exposures of the early Cretaceous sediments which
71 document intra-plate continental deposition during the early break-up of India from
72 Gondwana. It follows that the Ghaggar-Hakra Formation is likely to be the time and
73 depositional-equivalent of the Lower Cretaceous fluvial Himatnagar Sandstone of the
74 Cambay Basin (Bhatt *et al.*, 2016; Mohan, 1995; Mukherjee, 1983), the fluvial to marine

75 Nimar Sandstone of the Narmada Basin (Ahmad, 1988), the fluvial to coastal and deltaic Bhuj
76 Formation of the Kachchh Basin (Biswas, 1987; Desai & Desai, 1989; Akhtar & Ahmad, 1991),
77 the predominantly fluvial Dhrangadhra Group of the Than Basin in Saurashtra (Casshyap &
78 Aslam, 1992) and the fluvial Lumshiwai and Goru and marine-coastal Sembar successions of
79 the Central and Southern Indus basins of Pakistan (Ahmad *et al.*, 2012; Ahmad & Khan, 2012;
80 Khalid *et al.*, 2014; Zaigham & Mallick, 2000). These basin margin early Cretaceous
81 sediments are likely to be contemporary with rifting between Madagascar and India (Bastia
82 *et al.*, 2010; Reeves, 2014; Torsvik *et al.*, 2000) and separation of the Seychelles micro-
83 continent from Greater India (Eagles & Hoang, 2014).

84 Therefore, the Ghaggar-Hakra Formation and these isolated occurrences of fluvial sediments
85 are important in reconstructing the Lower Cretaceous depositional palaeogeography of the
86 north-western Indian Plate. Identification and detailed characterisation of a well-preserved
87 fluvial succession of Lower Cretaceous age in the Barmer Basin not only has significant
88 implications for the evolution of the basin, but also for potential reservoir distribution and
89 hydrocarbon potential of early Cretaceous sediments in the subsurface across the northern
90 Indian Plate.

91 Here, a comprehensive description and interpretation of the Lower Cretaceous Ghaggar-
92 Hakra Formation exposed in the Sarnoo and adjacent hills close to the settlements of Sarnoo
93 (also known as Sarnu or Saranu), Karentia and Nosar, Rajasthan (Fig. 1B) is presented as a
94 basis for re-evaluating the early Cretaceous palaeogeography of the northern Indian Plate
95 margin. Detailed sedimentary logging, combined with geometrical analysis of large-scale,
96 two-dimensional inclined exposures, are used to characterise and interpret the evolution of

97 the fluvial succession. Variations in fluvial style and the controls upon them are discussed,
98 along with the implications for the evolution of the Barmer Basin and its palaeogeographical
99 setting in the early Cretaceous Period during the early separation of India Plate from
100 Gondwana.

101 **Geological setting**

102

103 The WIRS (Fig. 1A) includes, from south to north, the Narmada, Cambay, Kachchh (Kutch)
104 and Barmer basins (Akhtar & Ahmad, 1991; Biswas, 1987; Pandey *et al.*, 2009; Rai *et al.*,
105 2013). The formation of the WIRS was initiated in the mid to late Jurassic Period by the
106 break-up of Gondwana as the eastern part, including the terranes of Greater India,
107 Madagascar and Antarctica, separated from West Gondwana (Africa) in response to the
108 development of the Mozambique and Somali proto-oceans west and north of Madagascar
109 and India (Reeves & DeWit, 2000; Reeves, 2014). Strike-slip reactivation of pre-existing
110 Proterozoic structures (from tectonic inheritance: Misra & Mukherjee, 2015) in the Jurassic
111 produced the Kachchh Basin (Biswas, 1982, 1999). By early Cretaceous times, development
112 of the Mozambique and Somali proto-oceans gave way to sea-floor spreading between the
113 Greater Indian and Antarctic continents (Eagles & Hoang, 2014; fig. 3 of Bladon *et al.*,
114 2015b). Consequently, the northward movement and anticlockwise rotation of the Greater
115 Indian continent occurred as break-up progressed (Chatterjee *et al.*, 2013; Storey *et al.*,
116 1995; Torsvik *et al.*, 2000) forming a series of interlinked failed rifts that constitute the WIRS.
117 Although the Jaisalmer and Indus basins are well known to have a late Gondwanan origin,
118 the relationship between the Cretaceous sediments of the WIRS, the Jaisalmer and Indus
119 basins remains obscure as it is patchily preserved across the northern margin of the Indian

120 Plate below the Deccan Traps (Ahmed & Amad, 1991; Akhtar & Ahmad, 1991; Chowdhary,
121 1975; Jaitly & Ajane, 2013; Misra & Mukherjee, 2017; Khosla *et al.*, 2003; Raju, 1968;
122 Sharma, 2007; Sheth, 2007) and the geometry and extent of the associated rifts are poorly
123 documented. That said, preservation of isolated fluvial Lower Cretaceous sediments clearly
124 suggests the presence of an established rift system through the north-western Indian Plate
125 prior to the onset of the main Deccan eruptions around 64 Ma in the Danian (Mukherjee *et*
126 *al.*, 2017). Regional palaeogeographical reconstructions (Biswas, 1999; Chatterjee *et al.*,
127 2013) also include continental rift basins between India, Madagascar and the Seychelles
128 microcontinent, although the geometry of these rifts and their sedimentary fills are very
129 poorly described (see Plummer & Belle, 1995).

130

131 The Barmer and Cambay basins, together with the Sanchor sub-Basin that separates them,
132 form a present day generally north-northwest trending rift 'arm' of the WIRS extending up to
133 600 km into northwestern India from the Gulf of Khambhat (Fig. 1A). The Barmer Basin is a
134 200 km long, <40 km wide, 6 km deep, failed continental rift (Bladon *et al.*, 2015a; Biswas,
135 1982; Compton, 2009; Dolson *et al.*, 2015) (Fig. 1B) containing continental sediments (Fig.
136 2A; Compton, 2009; Dolson *et al.*, 2015; Sisodia & Singh, 2000). A comparable rift system,
137 generally known as the Thar or 'Lower Indus' rift (Ahmed & Ahmad, 1991; Zaigham &
138 Mallick, 2000; Zaigham *et al.*, 2012) and specifically including the Panno-Aqil Graben,
139 extends northwards into Pakistan south of the Mari-Kandkot High and east of the Jacobabad
140 High (Ahmed & Ahmed, 1991) and probably represents the continuation of the WIRS.

141

142 Subsidence and sedimentation along the WIRS presumably continued contemporaneously
143 with rifting of the Seychelles microcontinent and eruption of the Deccan volcanics at the

144 Cretaceous-Palaeogene boundary ~65 Ma (Collier *et al.*, 2008; Eagles & Hoang, 2014;
145 Ganerød *et al.*, 2011; Plummer *et al.*, 1998). The exact causes of this extension remain
146 equivocal, with many authors citing the migration of the western margin of India over the
147 Reunion Plume (Morgan, 1971; Plummer & Belle, 1995; Simonetti *et al.*, 1995), even though
148 the present-day Reunion Plume impinges on a remnant of continental crust (Torsvik *et al.*,
149 2013).

150

151 Post-Deccan subsidence was concentrated along the Cambay-Barmer rift where some 6 km
152 of alluvial through to lacustrine environments of Palaeogene and Neogene age have
153 accumulated (Roy & Jokhar, 2002; Sisodia & Singh, 2000; Tabaei & Singh, 2002; Tripathi *et*
154 *al.*, 2009). These sediments have developed under a tropical to sub-tropical climate (Ali &
155 Aitchison, 2014; Chatterjee *et al.*, 2013; Hallam, 1985) as the Indian Plate migrated
156 northwards to its present-day position.

157 The Barmer Basin

158 Rifting in the Barmer Basin resulted from two distinct non-coaxial extensional events (Bladon
159 *et al.*, 2015b; Dasgupta & Mukherjee, 2017). An earlier northwest to southeast extensional
160 phase, oblique to the present orientation of the basin, was followed by dominantly
161 Palaeogene northeast to southwest extension (Bladon *et al.*, 2015b). Together, these two rift
162 events produced an asymmetrical half-graben in the north and a more symmetrical graben
163 in the south. Seismic data from the Barmer Basin indicates that pre-Deccan rifting is present
164 along the full extent of the basin with stratigraphical thickening being pronounced on the
165 present-day eastern margin (Dolson *et al.*, 2015).

166

167 Basement rocks of the Precambrian Malani Igneous Suite are unconformably overlain by
168 clastic fluvial sediments of the Jurassic Lathi Formation and the Lower Cretaceous Ghaggar-
169 Hakra Formation (Fig. 2A). Eastwards the Ghaggar-Hakra Formation onlaps the Karentia
170 Volcanic Formation (Fig. 2A), consisting predominantly of microcrystalline and plagioclase-
171 phytic basalts (Roy & Jokhar, 2002) which erupted in response to initial rifting between east
172 and west Gondwana (Bladon *et al.*, 2015a; Storey *et al.*, 1995; Reeves & DeWit, 2000).
173 Previous authors have ascribed all three of these formations to a 'pre-rift succession'
174 (Biswas, 1987; Compton, 2009; Roy & Jokhar, 2002).

175

176 Syn-rift strata are ascribed to the Palaeogene Mallinath Group and the early part of the
177 Eocene Jagmal Group (Fig. 2A). Earliest syn-rift strata of the Mallinath Group comprise acidic
178 pyroclastics and basaltic lavas of the Raageshwari Volcanic Formation erupted
179 predominantly in the centre of the basin (Compton, 2009), whilst contemporary alluvial fan
180 sediments (the Dhandlawas Formation) were deposited along the western margin, adjacent
181 to major fault scarps (Dolson *et al.*, 2015). From Maastrichtian to Thanetian times, braid-
182 plain fluvial and alluvial systems of the Fatehgarh and Barmer Hill formations dominated
183 with alluvial fan deposition (Jogmaya Formation) along the western faulted margin and
184 flanking horsts within. Regional uplift removed the youngest Barmer Hill strata to produce a
185 widespread unconformity across the basin before deposition resumed in Ypesian times
186 (Jagmal Group). Lacustrine systems (Dharvi Dungar Formation) dominated during the early
187 Jagmal Group giving way to swamp clastics of the Thumbli and Akli formations by Lutetian
188 times exhibiting minor marine incursions.

189

190 Post-rift subsidence and in-fill began in Lutetian times with lacustrine sediments of the
191 Nagarka Formation (Dolson *et al.*, 2015). A period of uplift coincident with collision of the
192 Indian and Eurasian plates developed the regional base Miocene unconformity, before
193 deposition of the fluvial and alluvial Neogene Jagadia and Uttarlia formations of the Rawal-
194 Umed Group (Najman *et al.*, 2018).

195

196 The Ghaggar-Hakra Formation

197 In the Sarnoo Hills, a succession of fluvial sediments unconformably overlay volcanic rocks of
198 the Karentia Volcanic Formation and, in places, the Malani Igneous Suite (Fig. 2B; Baksi &
199 Naskar, 1981; Compton, 2009; Mishra *et al.*, 1993; Sisodia & Singh, 2000). The formation is
200 ~100 m thick at outcrop (Mishra *et al.*, 1993) and comprises three distinct, quartz-rich, fluvial
201 channel belt sandstone packages separated by ~30 m of variegated white and red coloured,
202 horizontally-laminated and cross-laminated sands, with rhizoliths and soft-sediment
203 deformation structures (Bladon *et al.*, 2015a), attributed to deposition on a fluvial floodplain
204 (Bladon *et al.*, 2015a, b). The sandstone packages have been assigned informal
205 lithostratigraphical status and named (in ascending order): the Darjaniyon-ki Dhani, Sarnoo
206 and Nosar sandstones (Fig. 2B; Bladon *et al.*, 2015a, b).

207

208 The Darjaniyon-ki Dhani Sandstone comprises poorly sorted and clast-supported lithic
209 arenites along with coarse sand to pebble-grade conglomerates attributed to deposition in
210 an immature, braided system with a high sediment load (Bladon *et al.*, 2015a). The Sarnoo
211 Sandstone comprises cyclic, well-sorted, fine to medium-grained, quartz arenites with
212 regular cross-bedded sets (Sisodia & Singh, 2000) and deposited in a mobile meandering

213 system (Bladon *et al.*, 2015a). The Nosar Sandstone caps the formation at outcrop and
214 comprises medium to coarse-grained sands and granule-grade conglomerates with cross-
215 bedded sets and channel geometries with erosive bases, typical of deposition in an actively
216 migrating braided fluvial system (Bladon *et al.*, 2015a).

217

218 Plant leaves (*Phlebopteris athgarhensis* Jain, *Ptilophyllum acutifolium* Morris and
219 *?Sphenopteris* sp.; Baksi & Naskar, 1981; Compton, 2009; Rajanikanth & Chinnappa, 2016)
220 are present within the formation and are characteristic of the *Dictyozamites – Pterophyllum –*
221 *Anomozamites* Assemblage (8th) zone (Dev, 1987; Rajanikanth & Chinnappa, 2016). Together
222 with trisaccate pollen (*Podocarp Microcachrydites* spp., *Cyclusphaera* spp.), they date the
223 Ghaggar-Hakra Formation to the Lower Cretaceous. Further constraints on the earliest age
224 of the formation are provided by an Aptian (120 Ma) date for the underlying basalts of the
225 Karentia Volcanic Formation (Sharma, 2007) and basaltic intrusions of Deccan age (68.57 ±
226 0.08 Ma; Basu *et al.*, 1993) constrain the youngest age of these sediments; indicating the
227 formation is Aptian to Albian age.

228 **Dataset, methods and field area**

229 The Ghaggar-Hakra Formation is exposed in a series of three low-lying, fault-bounded hills
230 separated by a peneplained surface covered in modern desert deposits near the village of
231 Sarnoo. Progressive down-stepping of the faulted blocks toward the west and north provides
232 excellent exposures that can be correlated providing continuous, composite vertical
233 sections. Extensive quarrying provides continuous lateral exposure of the sediments in the
234 scarp slopes of these hills. The dataset consists of 114 detailed sedimentary logs (Fig. 3) and
235 53 detailed two-dimensional panels providing correlation and geometries between the logs.

236 **Sedimentology of the Ghaggar-Hakra Formation**

237 The details of lithofacies are given in Table 1 and Fig. 3. Eight architectural elements (Table 2
238 and Figs 4, 5 and 6) are identified and summarised below with the bounding surface
239 terminology of Miall (1985, 1988).

240 Channel element – Ch

241 *Description*

242 These 'U'-shaped elements (Table 2) – laterally up to ~25 m and ~7 m thick – are bound by
243 sharp, sometimes erosional, convex-down 5th order surfaces at their bases, and generally
244 planar and concordant 4th order surfaces at their tops. The basal 5th order bounding surface
245 erodes other elements of this type (Ch), overbank (Ob), or channel margin (Cm) elements
246 but the 4th order surface, where preserved, is gradational over approximately 2 m into
247 overlying point bar (Pb) or overbank (Ob) elements. Typically, the full geometry is not
248 preserved, eroded by younger channels (Ch), channel margins (Cm), gravel bars (Gb), point
249 bars (Pb) or sheet flows (Sf; Figs 4A, 5A and 6A).

250 The 5th order surface is immediately overlain by the pebble-grade quartz clasts of grain-
251 supported conglomerate (G) characterised by indistinct cross-bedding. The conglomerate is
252 typically overlain by cross-bedded sandstone (Stx, Sx) in sets (30 cm thick) and co-sets (50 –
253 95 cm thick) bound by 1st to 3rd order surfaces. The contact between the basal conglomerate
254 and sandstone is sharp, generally with pebble-grade lenses within the toe-sets of the
255 lowermost cross-bedded sets. Sporadically, convolute bedding, tree stumps and rip-up clasts
256 are preserved, and packages of structureless sand (Sm) occur between sets of cross-bedded

257 sandstone (Stx, Sx). Where preserved, the upper half of the element comprises horizontally-
258 laminated sandstone (Sh) and cross-laminated sandstone (Scl) in sets climbing at 5°. These
259 sediments are overlain by mottled, bioturbated, very fine-grained pedogenic sands (Sp; Fig.
260 6A).

261 *Interpretation*

262 These elements are interpreted to represent small-scale, erosively based, fluvial channels.
263 The initial conglomeratic deposits overlying the channel base indicate high-energy flow with
264 significant bedload transport. Pebble lenses are concentrated in areas marking the thalweg,
265 indicating unsteady flow with localised periods of scour and fill (Froude *et al.*, 2017). Cross-
266 bedded sandstone (Stx, Sx) sets record the development and migration of lower flow regime
267 bedform trains and barforms, generally migrating towards the south-west. The irregular
268 nature of the sets and the range of bounding surfaces (along with convolute bedding, tree
269 stumps and rip-up clasts where preserved) suggests flow variability and reactivation of
270 bedforms and barforms.

271 Above this, the sediments (Scl, Sr, Sp) represent a decrease in energy as the flow wanes and
272 ripple-scale bedforms develop in trains and migrate. Bioturbation and structureless sands
273 below the 4th order surface most likely represents the final stages of sedimentation within
274 shallow, largely stagnant waters, followed by pedogenesis.

275 Channel margin element – Cm276 *Description*

277 These tabular to wedge-shaped elements – up to 5 m high and 10 m long – are bound by
278 planar 5th order surfaces at their bases and planar 4th order surfaces at their tops (Table 2).
279 5th order surfaces are sharp and typically concordant with the underlying and overlying
280 sediments. Typically, they merge laterally with 5th order surfaces of channel elements and
281 become erosional. Sporadically, basal surfaces are replaced by a slightly gradational contact
282 from the underlying channel elements (Ch). Upper 4th order surfaces are sharp with the
283 overlying sediments of gravel bar (Gb), point bar (Pb), sheet flow (Sf) or overbank (Ob)
284 elements.

285 Bases are overlain by stacked, sub-critically climbing sets (30 cm) and co-sets (95 cm) of
286 planar cross-bedded sandstone (Sx) bounded by 1st to 3rd order surfaces. Above these, sets
287 of cross-laminated sandstone (Scl) climb sub-critically at 5°. Capping the elements are
288 deposits of fine-grained, horizontally-laminated sandstone (Sh) and pedogenic facies (Sp, Ip;
289 Figs 4B, 5B and 6B).

290 *Interpretation*

291 These elements are interpreted to represent the deposition of sediments on the channel
292 margin as flooding occurs. Sets of cross-bedded sandstone (Sx) and cross-laminated
293 sandstone (Scl) represent the development and migration of dune- and ripple-scale
294 bedforms as the flow overtops the channel on to the floodplain and wanes (O’Conner *et al.*,
295 2003; Wakefield *et al.*, 2015). The presence of horizontally-laminated sandstone suggests

296 periodic episodes of upper flow regime conditions as water moves from the restricted
297 channel to an unrestricted floodplain (Brierley *et al.*, 1997). Mottled sands and silts with
298 poorly preserved bedding possibly indicate destruction of primary depositional fabrics by
299 vegetation.

300 Gravel bar element – Gb

301 *Description*

302 These lenticular elements – up to 75 m long and 4 m thick – are bound by sharp and erosive
303 5th order surfaces at their bases, eroding into channel (Ch) or overbank (Ob) elements, and
304 sharp or gradational 4th order surfaces into the channel, point bar or overbank elements (Ch,
305 Pb, Ob; Figs 4C, 5C and 6C, Table 2). 5th order surfaces are laterally extensive and can
306 transition laterally into 5th order surfaces at the base of channel elements (Ch).

307 Matrix-supported conglomerates (M) and / or clast-supported conglomerates (G)
308 immediately overly the bases. Matrix-supported conglomerates (M) comprise rounded
309 quartz clasts and extraformational lithics, supported in a matrix of very fine to fine-grained
310 sandstone. Sporadically, indistinct foresets of cross-bedding are present. Clast-supported
311 conglomerates (G) comprise poorly sorted but rounded pebbles of quartz and
312 extraformational lithic clasts with sporadic and indistinct cross-beds.

313 The upper third comprises either massive sandstone (Sm) or horizontally-laminated
314 sandstone (Sh) facies (Fig. 6C), exhibiting sharp contacts with the underlying sediments. The
315 massive sandstone is moderately to poorly sorted with numerous quartz clasts. The clasts
316 are typically distributed randomly, but sporadically form indistinct horizontal layers. The

317 horizontally-laminated sands are up to 9 mm thick but thin upwards. The full succession is
318 rarely preserved and conglomerates (M, G) dominate.

319 *Interpretation*

320 Highly erosional 5th order surfaces typically contiguous with those of channels and
321 conglomeratic sediments indicate gravel bar deposition primarily by bedload transport
322 under high-energy conditions (Froude *et al.*, 2017). This is likely to have occurred along the
323 bases of developing channels with long axes of bars parallel to the channel. Grainsize is not
324 conducive to producing bedforms, and a high sediment load promotes rapid deposition that
325 further suppresses their development (Bridge & Best, 1988). Where sediment load is reduced,
326 deposits grade from matrix to clast-supported with sporadic and poorly developed cross-
327 bedding indicating some migrating bedforms (Blair & McPherson, 1994) and implying
328 transient gravel bar movement (Figs 4C, 5C and 6C; c.f. Bridge 1993).

329

330 Massive and horizontally-laminated sandstone represents deposition in shallow water on
331 top of the developing barforms. Horizontally-laminated sandstone was deposited under
332 upper flow regime conditions (Ghazi & Mountney, 2009) when the gravel bars were fully
333 submerged. Massive sandstone represents deposition when the top of the bar was at
334 surface or slightly emergent, and stationary waters allow suspension fall out (Banham &
335 Mountney, 2013; Jones & Rust, 1982).

336 Chute channel element – Cc337 *Description*

338 These small, symmetrical 'U'-shaped elements are up to 70 cm in height and no more than
339 2 m wide (Table 2). Their lower 5th order bounding surfaces are convex-down and erosional
340 into either point bar (Pb) or overbank (Ob) elements. Upper 4th order surfaces are generally
341 gradational into the overbank elements (Ob) over a thickness of 50 cm (Figs 4D, 5D and 6D).

342 Internally, the succession fines upwards from grain-supported conglomerates (G) composed
343 of quartz clasts, through massive sands and silts (Sm, Im) containing quartz clasts up to
344 5 mm. This succession culminates in parallel-bedded sands and silts forming ~50 cm thick
345 packages with individual beds ranging between 10 cm and 15 cm thick and the horizontally-
346 laminated sandstone (Sh) with packages up to 80 mm with laminations up to 9 mm thick.
347 Capping this element are bioturbated, rooted, pedogenically modified fine-grained sands
348 and silts (Sp, Ip). Typically, the succession is fully preserved, but sporadically, granule-grade
349 conglomerates (G) pass straight into pedogenically modified sands and silts (Sp / Ip)
350 producing a strongly bimodal grainsize profile.

351 *Interpretation*

352 The 'U'-shaped geometries and their erosional lower bounding surfaces are indicative of
353 small-scale channels. Conglomerates (G) consisting of locally reworked material immediately
354 overlying 5th order surfaces suggest initial deposition of sediments in a high-energy flow
355 cutting channels (Bordy *et al.*, 2004). Subsequently, flow waned rapidly to stagnant
356 conditions with a high sediment load promoting deposition of massive sands and silts (Sm,

357 lm; Martin & Turner, 1998). Where present, parallel-bedded and horizontally-laminated
358 sandstone (Sb, Sh) may suggest periods of extended and fluctuating upper flow regime
359 conditions prior to rapid waning (Wakefield *et al.*, 2015). In other examples, flow waned
360 rapidly to stagnant water, depositing a strongly bimodal grainsize (Martin & Turner, 1998).

361 The strong spatial association between these elements and point bar elements (Pb), coupled
362 with palaeocurrents that are generally perpendicular to the main channel system, suggest
363 small-scale, high-energy chute channels formed during flood conditions (Ghinassi, 2010;
364 Wakefield *et al.*, 2015). During flooding, sediment load is high, increased discharge promotes
365 'short-cutting' of the system across meanders, and energy levels wane rapidly to promote
366 rapid and structureless deposition (Wakefield *et al.*, 2015). Further evidence for this
367 interpretation is provided by the presence of locally reworked quartz clasts most likely
368 derived directly from the main channel system. Pedogenic sands and silts (Sp, Ip) represent
369 bioturbation and reworking of later stage sedimentation. The geometries of these elements
370 suggest 'low sinuosity' chute channels comparable to the 'type 1' chute channel of Ghinassi
371 (2010).

372 Point bar element – Pb

373 *Description*

374 These wedge-shaped elements (Table 2), up to 4 m thick and a maximum of 15 m wide, are
375 bound by lower 5th order surfaces that are sporadically slightly erosional but are generally
376 concordant with underlying strata and typically extend laterally into the base of a channel
377 (Ch). Upper 4th order surfaces, where preserved, are concordant with sediments of overbank

378 (Ob) and / or channel margin (Cm) elements. Typically, the upper parts of these elements are
379 not preserved because of erosional down-cutting by chute channel (Cc), channel (Ch) or
380 sheet flow (Sf) elements (Figs 4E, 5E and 6E).

381 Overlying the 5th order surfaces are co-sets (95 cm thick) of planar cross-bedded sandstone
382 (Sx) comprising sets of up to 30 cm thick that are interbedded with 2 m thick co-sets of low-
383 angle cross-bedded sandstone (Sla). This succession generally fines upward. Sets of both
384 facies are bound by 1st or 2nd order surfaces and sporadically truncated by 3rd order surfaces.
385 Capping the elements is cross-laminated sandstone (Scl) forming individual sets up to 5 cm
386 thick with internal structures disrupted by meniscate trace fossils of *Taenidium* or *Beaconites*
387 (Gowland *et al.*, 2018).

388 *Interpretation*

389 Elements of this type are interpreted to represent the deposits of laterally accreting point
390 bars. Multiple sets and co-sets of cross-strata decreasing in size from dune to ripple scale
391 (Sx, Sla, Scl) are the product of migrating bedforms within the lower flow regime (Ghazi &
392 Mountney, 2009; Jackson, 1976), this, combined with the reduction of grainsize indicates a
393 waning flow. The complex and varied geometry of sets and co-sets and numerous bounding
394 surfaces of varying scales suggest dominantly lateral but slightly down-stream migrating
395 barforms. 3rd order surfaces suggest frequent reactivation and meniscate trace fossils
396 towards the top suggest calm, possibly emergent, conditions with ripple-lamination
397 representing wash-over of the bar (Bridge *et al.*, 1995). 5th order bounding surfaces grading
398 laterally into the bases of channel elements (Ch) and the spatial association of these two

399 elements demonstrate an evolutionary relationship between them suggesting attachment of
400 the bar to the channel.

401 Sheet flow element – Sf

402 *Description*

403 These sheet-like tabular elements (Table 2), with a thickness of ~0.5 m, are bound by lower
404 5th order surfaces that are convex-down and erosive. Where the elements are fully
405 preserved, 4th order surfaces bound their tops and separate them from the overlying
406 overbank (Ob) elements. However, the tops of the elements are typically marked by erosive
407 surfaces at the bases of successive elements of sheet flow (Sf), or at the bases of channel
408 (Ch), chute channel (Cc) or point bar (Pb) elements (Figs 4F, 5F and 6F).

409 Facies of these elements form an ordered succession. Beds up to 30 cm thick of parallel-
410 bedded sandstone (Sb) fine and thin upward into beds of horizontally-laminated sandstone
411 (Sh). Overlying these are sets (10 cm) of rippled sandstone (Srha), climbing super-critically up
412 to 30°, and stacked 30 cm cosets of cross-laminated sandstone (Scl) climbing sub-critically at
413 5°. Pedogenic sandstone and siltstone (Sp, Ip) display mottled textures, and contain fossil
414 leaf imprints along with meniscate trace fossils typical of *Taenidium* or *Beaconites* (Gowland
415 *et al.*, 2018).

416 *Interpretation*

417 Deposition of subaqueous facies above 5th order surfaces with sheet-like geometries
418 indicates a largely unconfined flow (Blair, 2000). Upper flow regime conditions initially

419 prevailed, depositing parallel-bedded sandstone and horizontally-laminated sandstone (Sb,
420 Sh). Waning occurred rapidly to lower flow regime conditions depositing rippled sandstones
421 (Srha, Scl; Hjellbakk, 1997) indicating bedform development and migration. Variations in
422 climbing angle suggest variations in sediment load, flow competency and capacity (Blair,
423 2000; Hampton & Horton, 2007; Hunter 1977a, b). Pedogenic facies with high levels of
424 bioturbation and abundant plant remains implies times of depositional quiescence (Bromley
425 & Asgaard, 1979, 1991; Buatois & Mangano, 2002).

426 The relationships between sheet flows, channels and bars (Sf, Ch, Pb and Gb) suggest that,
427 whilst largely 'unconfined' (Banham & Mountney, 2013), the sheet flows may be restricted
428 to the lateral extent of active channel belts and most probably represent times of high
429 discharge when channels were filled to capacity.

430 Overbank element – Ob

431 *Description*

432 These elements are dominantly tabular (Table 2), up to 1.5 m thick and 2 km in lateral extent
433 and bound at their tops and bottoms by planar 4th order surfaces except where tops are
434 eroded by overlying channel (Ch) or gravel bar (Gb) elements. Lower boundaries can be
435 sharp where overbank elements overlay gravel bars (Gb), or gradational where they overlay
436 point bar or sheet flood (Pb, Sh) elements (Figs 4G, 5G and 6G).

437 The facies occur in any order, but when massive sandstone and siltstone (Sm, Im) and / or
438 horizontally-laminated sandstone (Sh) are present they typically overlay the 4th order
439 surface, interbedded in an apparently random manner by individual sets of cross-laminated

440 sandstone (Scl). When present, together these facies account for no more than 15% of the
441 element with the remainder comprising pedogenic facies (Sp, Ip, Ihe). Pedogenic facies are
442 dominantly red, and contain abundant granular peds (Retallack, 1988) between 2 cm and 3
443 cm long, along with grey to white patches of generally coarser grain. Abundant orange
444 goethite-rich rhizoliths reach lengths of 15 cm (Fig. 7), and carbonate cemented rhizoliths
445 reach lengths of 1 m (Fig. 4G) along one particular horizon. All facies are remarkably fissile,
446 and rare root structures and soils slickensides can be found throughout.

447 *Interpretation*

448 The physical dimensions and particularly the lateral extents indicate sediments of
449 unconfined overbank floods. The facies indicate sub-aqueous upper (Sh Sm) and lower flow
450 regime conditions with limited bedform development or migration (Scl) and occasional
451 suspension settlement (Sm, Im). Facies displaying granular peds and extensive colour
452 mottling indicate significant bioturbation (Sp, Ip, Ihe; Retallack, 1988; Tennvassås, 2018),
453 subaerial exposure and palaeosol formation (Retallack, 1988; 1990).

454 Elements of this type typically overlie one-another, with little to no erosion, and likely
455 represent cumulative soil growth on a floodplain supplied regularly with sediment from
456 flooding (Kraus, 1999; Kraus & Aslan, 1999). The rhizoliths indicate floodplain areas were
457 imperfectly to poorly drained soils (Kraus & Hasoitis 2006) suggesting they were seasonally
458 wet (Retallack 1990).

459 Pond element – Po460 *Description*

461 These elements form lenticular bodies – up to 2 m thick and 50 m wide (Table 2). The lower
462 and upper boundaries are both 4th order surfaces and this element grades into the overbank
463 (Ob) element over ~30 cm.

464 Facies do not form regular definable successions, but where present cross and horizontally-
465 laminated sandstones (Scl, Sh) are typically preserved near element bases, followed by
466 massive fine-grained sandstone and siltstone (Sm, lm), with pedogenic (lp) and haematitic
467 siltstone (lhe) dominating.

468 *Interpretation*

469 Elements of this type are interpreted as small ponds of limited lateral extent developed on
470 the overbank areas. Horizontally-laminated sandstone, massive sandstone and massive
471 siltstone (Sh, Sm, lm) indicate that sediment deposition was dominated by suspension
472 settlement. Sporadic cross-lamination (Scl) indicates development and migration of small
473 ripple-scale bedforms when pond levels were recharged by overbank flooding. Wind shear
474 on standing water combined with localised current turbulence formed symmetrical,
475 asymmetrical and interference ripple patterns (Sr; Wilson, 1993). The development of soils
476 (Sp, lp, lhe) as ponds dried-out obliterated many primary bedding structures.

477 **Depositional Model for the Ghaggar-Hakra Formation**

478 All the field observations support the presence of a fluvial system where the transport and
479 deposition of sediment takes place within erosive channels by the development of in-
480 channel barforms (Ch), accompanied by bedload transport (Gb). The fluvial channels are
481 accompanied by laterally accreting bars (Pb) with chute channels (Cc), channel-margin
482 sediments (Cm) and sheet flows (Sf). The elements are arranged to form distinct 'channel
483 belt' depositional elements (terminology of Grotzinger *et al.*, 2005; Posamentier & Kolla,
484 2003). Each belt is separated by 'floodplain' depositional elements dominated by fine-
485 grained sediments deposited in bodies of standing water (Po) or by unconfined flooding
486 (Ob). Three channel belt depositional elements are recognised that correspond to the
487 informal lithostratigraphical subdivisions of Bladon *et al.* (2015a, b): the Darjaniyon-ki Dhani,
488 Sarnoo and Nosar sandstones. Conceptual facies models for these depositional elements are
489 presented in Figures 8, 9 and 10 along with a description of the key features and element
490 relationships that define them. An interpretation of each is given below.

491 The Darjaniyon-ki Dhani Sandstone is dominated by stacked and amalgamated channels and
492 gravel bars indicating a highly mobile, bedload-dominated system where barform migration
493 was transient (Best *et al.*, 2003; Bridge, 1993). Transient bars, coupled with a scarcity of
494 completely preserved elements, a range of grainsizes and rare preservation of overbank
495 suggests a highly avulsive system perhaps controlled by frequent changes in energy (Cant &
496 Walker, 1978). The dominance of gravel bar elements (Gb) comprising sediments of debris-
497 driven processes (Tables 1 and 2) indicates a high sediment load (Gulliford *et al.*, 2014; Lowe,
498 1988; Mather *et al.*, 2008) representing a bedload-dominated, low sinuosity fluvial system
499 (fig. 8 of Miall, 1985).

500 The sediments of the Sarnoo Sandstone are dominated of stacked and amalgamated
501 transient gravel bars in the initial deposits indicating a significant degree of channel avulsion.
502 Sinuosity and stability increase up section to develop channels of stable flow with associated
503 point bars and chute channels (Ielpi & Ghinassi, 2014; fig. 13 of Miall, 1985). However,
504 discharge is still sufficiently irregular to cause sheet flows (Sf) and support ponding on the
505 floodplain; overall this system represents a mixed load, high sinuosity fluvial system (fig. 11
506 of Miall, 1985).

507 The Nosar Sandstone displays channels with some degree of stability but separated by
508 transient bars. The system was influenced by avulsion and flooding (Best *et al.*, 2003; Bridge,
509 1993). Sparse preservation of the overbank may indicate limited and patchy development, or
510 poor preservation because of frequent fluvial avulsion. All features indicate a bedload
511 dominant, low sinuosity fluvial system (fig. 9 of Miall, 1985).

512 Channel belt elements are separated by significant sections of floodplain sediments (Fig. 2B),
513 that formed through cumulative soil growth and were likely imperfectly to poorly drained
514 due to being seasonally wet. Cyclicity suggests regular flooding which supplied the
515 floodplains with new sediment and recharged ponds, probably a consequence of channel
516 instability caused by variations in discharge and sediment load. The thickness of preserved
517 floodplain suggests that the channel belts themselves were reasonably stable for significant
518 periods.

519 The change in fluvial style from the Darjaniyon-ki Dhani to the Sarnoo sandstones,
520 particularly the increase in sinuosity and the decrease in the dominance of bedload

521 transport, indicates progressive maturing of the Ghaggar-Hakra fluvial system through time
522 (Schumm, 1981). This interpretation is supported by evidence for less flooding and fewer
523 floodplain ponds up-section. However, a decrease in sinuosity from the Sarnoo to Nosar
524 sandstones, coupled with an increase in the proportion of bedload, an increase in bedform
525 and barform migration, and stacking at all scales is atypical of increasing fluvial maturity (Fig.
526 11) and indicates rejuvenation of the whole system.

527 **Discussion**

528 The Ghaggar-Hakra succession

529 The Ghaggar-Hakra Formation records the maturing evolution of an early Cretaceous fluvial
530 system, followed by a sudden rejuvenation, preserved on an atypical relay ramp on the
531 margin of the Barmer Basin. Dating indicates the succession is of Aptian-Albian age.
532 Deposition of fluvial sediments always represents the complex interplay between the
533 intrinsic processes of sediment transport and deposition and allogenic-controls acting at a
534 variety of spatial and temporal scales (Leeder, 1993). Notwithstanding the constraints of the
535 limited spatial extent of the outcrop available in this study, the relative dominance of broad-
536 scale allocyclic-controls of climate and tectonics (Gawthorpe & Leeder, 2000; Robinson &
537 McCabe, 2012) and the implications for the evolution of the Barmer Basin, warrant some
538 discussion as presented below.

539 During deposition of the Ghaggar-Hakra Formation initial rifting between India and
540 Madagascar had started but India and Madagascar remained a single island continent
541 (Biswas, 1987; Bladon *et al.*, 2015b). The WIRS was located ~40° south of the equator with

542 the Indo-Tethyan Ocean to the north, and the Aravalli Mountain Range and continental India
543 to the south, in a position between the subtropical arid and temperate climatic belts
544 (Acharyya & Lahiri, 1991; Chatterjee *et al.*, 2013). The abundance of plant remains in the
545 Ghaggar-Hakra Formation indicates that the floodplains were extensive and highly
546 vegetated, with abundant palms and conifers.

547 Studies and models from other fluvial systems evolving under well vegetated subtropical
548 regimes (Fielding *et al.*, 2009) display a range of characteristics that are like many of those
549 observed in the Ghaggar-Hakra, including stacked and amalgamated channels with
550 convolute bedding, tree stumps, imperfectly to poorly drained palaeosols (Kraus & Hasoitis
551 2006) and variable but significant amounts of floodplain deposition.

552 However, preserved floodplain thicknesses predicted from fluvial models for subtropical
553 conditions are notably thinner than those observed in the Ghaggar-Hakra (Fielding *et al.*,
554 2009), and the thick cyclic floodplain successions formed are attributed to periodic flooding,
555 the result of channel instability caused by temporal variations in discharge and sediment
556 load.

557 Changes in discharge and load may relate to local and / or regional controls of either
558 tectonics or climate. Given that the floodplain is very uniform, with a lack of internal
559 variation in its pedogenic nature, and that the Indian Plate was within the subtropical arid
560 and temperate climate belt (Chatterjee *et al.*, 2013; Scotese *et al.*, 2007; Scotese, 2011)
561 throughout the time of deposition; it is argued that climatic variation is unlikely to have had
562 a significant influence upon the fluvial rejuvenation. However, the climate did influence

563 overbank conditions and soil growth. Based on the palaeosol profile exhibited by overbank
564 elements, the floodplain likely formed oxiosols that imply it received at least 100 mm per
565 month of rain over 7 months of the year (Cecil & Dulong, 2013).

566 In the absence of climate control upon the rejuvenation of the fluvial system during Nosar
567 times, local or regional tectonics are the most likely influence on accommodation space and
568 sedimentation. Recent studies indicate a Mesozoic section is preserved in the subsurface up
569 to 6 km deep, in the centre of the Barmer Basin (Bladon *et al.*, 2015b; Kothari *et al.*, 2015)
570 and recognise a west-striking, pre-Palaeogene tectonic grain on the eastern margin (termed
571 the Saraswati Terrace Bladon *et al.*, 2015b) that is overprinted by the younger Palaeogene
572 extensional event. Bladon *et al.* (2015b) conclude that early northwest-southeast rifting is a
573 consequence of the trans-tensional structural regime that existed between Greater India
574 and Madagascar prior to their separation and the main phase of Deccan volcanic eruption.
575 The sedimentological work on the Ghaggar-Hakra presented herein indicates that this early
576 rift event did indeed influence depositional style and architecture as many of the
577 sedimentary characteristics of the Nosar Sandstone, and rejuvenation of the system, can be
578 explained by deposition on a tectonically subsiding continental alluvial plain.

579 However, there is no direct evidence from outcrop for stratal growth patterns in the
580 Ghaggar-Hakra, or for a strong relationship between fluvial drainage patterns and fault
581 geometry in the Darjaniyon-ki Dhani to Sarnoo sandstones, which is atypical as these
582 features are generally common in fluvial systems strongly controlled by contemporaneous
583 rifting (Gawthorpe & Leeder, 2000). Apart from the high-energy system recorded in the
584 initial deposits of the Darjaniyon-ki Dhani Sandstone, the succession through to the base of

585 the Nosar Sandstone exhibits progressive fluvial maturation suggesting stability and
586 quiescence. It is only during Nosar times that significant rejuvenation of the fluvial system
587 occurs and that can be attributed to tectonically induced changes in fluvial gradient (Bridge
588 & Leeder, 1979; Leeder, 1993; Schumm, 1993). Consequently, it is tempting to conclude that
589 the base of the Nosar Sandstone, rather than the base of the Ghaggar-Hakra, represents the
590 onset of active rifting in the Barmer Basin during the early northwest-southeast phase of
591 extension recognised by Bladon et al. (2015b). Alternatively, rift flank uplift accelerated
592 significantly at the base of the Nosar Sandstone, indicating syn-rift deposition during Early
593 Cretaceous times. This in turn implies high preservation potential for thick Early Cretaceous
594 fluvial successions within rifted fault blocks beneath the Palaeogene fill that likely have
595 significant potential for further hydrocarbon exploration.

596 Implications for Palaeogeography of the northwest Indian Plate in the Lower Cretaceous
597 Epoch

598

599 During Early Cretaceous times, clastic deposition across the northwest Indian Plate was
600 dominated by fluvial systems carrying sediment to coastal plains and deltas forming along
601 the edge of the Indo-Tethyan Ocean. In the Kachchh and the Middle and Lower Indus basins
602 the Lower Cretaceous Bhuj and Lower Goru formations are established reservoirs for
603 hydrocarbons (Ahmad *et al.*, 2012; Biswas, 1999; Mukherjee, 1983). However, Cretaceous
604 sediments are rarely exposed at outcrop across the Indian Plate, being preserved only within
605 rift basins or at basin margins, where they have been downfaulted and protected from the
606 effects of Palaeogene and Neogene uplift and erosion. Therefore, reconstructing even local
607 Cretaceous palaeogeography is difficult because of limited outcrop, and collation of

608 descriptions of the Lower Cretaceous sediments is required.

609 In addition to the Ghaggar-Hakra, Lower Cretaceous fluvial deposits are present in the
610 Kachchh (Aslam, 1992; Casshyap & Aslam, 1992) Cambay (Bhatt *et al.*, 2016; Mukherjee,
611 1983; Jana *et al.*, 2013) and Narmada (Akhtar & Ahmed, 1991; Racey *et al.*, 2016) basins and
612 shallow marine sedimentation occurred within the Kachchh (Racey *et al.*, 2016; Rai, 2006),
613 Jaisalmer (Singh, 2006), and Indus (Ahmad *et al.*, 2004; 2012) basins. There is also evidence
614 for ~1 km of Mesozoic sediments beneath the main Deccan volcanic pile as indicated by
615 geophysical mapping (Rajaram *et al.*, 2016; Rao *et al.*, 2015). Therefore, it is pertinent to ask
616 the following question, initially posed by Biswas (1999): was the Ghaggar-Hakra Formation
617 only deposited in the rift systems or was it widespread across the northwest Indian Plate?

618 The depth to top basement map for north-west India of Kothari *et al.* (2015) is used to
619 establish a detailed structural framework to depict the early Cretaceous rift systems which in
620 turn define the depositional systems and their distribution (Fig. 12). The extent, type and
621 distribution of the depositional systems are initially established from the Sarnoo Hills work,
622 together with published accounts of early Cretaceous outcrop and subsurface sediments,
623 before speculatively extrapolating facies following Walther's Law.

624 During Cretaceous times, the Indian Plate was rotated 90° clockwise with respect to its
625 present orientation (Fig. 12; Chatterjee *et al.*, 2013) so its leading edge comprised much of
626 present day Pakistan where the Lower Cretaceous sediments were deposited in coastal
627 embayments, deltas and shorefaces (Ahmad *et al.*, 2012; Smewing *et al.*, 2002). As India was
628 within the subtropical arid and temperate climate belt, the overall precipitation across India
629 was low to medium (1.5 – 12 cm/month; Chatterjee *et al.*, 2013). The FOAM palaeoclimate
630 simulations (Goswami, 2011; Scotese *et al.*, 2007; Scotese, 2011) indicate that the WIRS and

631 surrounding areas were comparatively dry and warm (17 °C) when compared to the east of
632 the India which is separated from them by the 600 km long Aravalli Mountain Range.

633 Along the northern leading edge of the Indian Plate, the coastal Sembar Formation
634 siliciclastics were deposited on top of an extensive carbonate platform (Khalid *et al.*, 2014).
635 This resulted from a gradual and long-term base-level rise leading to high-stand shedding
636 with the formation of a westerly prograding delta (the 'Goru Fan Delta'). An active longshore
637 drift and tidal influence restricted these sands to the east of the shelf where they formed a
638 ramp ~200 km wide (Ahmad *et al.*, 2004) that gradually deepened to the west and north (fig.
639 9 of Khalid *et al.*, 2014). The Goru Fan Delta fed by fluvial systems draining the northwest
640 Indian Plate built out into the marine embayment, across the Jaiasalmer Basin and the
641 Punjab Platform and is imaged on regional 2D seismic data (Fig. 12; Khalid *et al.*, 2014).
642 Consequently, the Lower Cretaceous shoreline, shelf edge positions and lateral shifts are
643 reasonably well-known across the north-west Indian Plate in south-central Pakistan (Khalid
644 *et al.*, 2014). Fluvial palaeocurrent directions across the Lower Goru Fan Delta are from the
645 east and southeast consistent with sources on the Indian Plate (Ahmad *et al.*, 2004). The
646 Ghaggar-Hakra Formation palaeocurrent directions, present day, are to the south-west (Figs.
647 7, 8, 9; Sisodia and Singh, 2000; Bladon *et al.*, 2015a) into the Barmer Basin reflecting their
648 location on a feeder relay ramp (Saraswati Terrace) into the rift and directed towards the
649 Cambay Basin. Therefore, it is possible to speculate that these sediments actually fed the
650 southerly part of the WIRS and potentially drained into a poorly known early Cretaceous rift
651 basin beneath the present-day Gulf of Khambhat. Early Cretaceous rivers draining the
652 Devikot High and the northern Aravalli Range likely supplied the Lower Goru and Sembar
653 formations across the Punjab Platform (Fig. 12).

654 This palaeogeographical reconstruction suggests a much more complex drainage system
655 than has previously been envisaged for the northern leading edge of the Indian Plate.
656 Upland deposits had a very low preservation potential which, compounded with later uplift
657 and widespread erosion preceding the Deccan volcanism, resulted in the disparate
658 preservation of fluvial early Cretaceous sediments. Along with Biswas (1999), it is proposed
659 here that most of the early Cretaceous sediments preserved in the WIRS are indeed
660 remnants of a syn-rift continental succession. By contrast, the coastal plain and deltaic
661 deposits of the Sembar-Lower Goru succession were much more regionally extensive at
662 deposition and accumulated along the Indo-Tethyan leading edge in coastal plain, deltaic
663 and shallow marine shoreface settings.

664 **Conclusions**

665 The outcrops at Sarnoo, Karentia and Nosar provide continuous sections and significant
666 insight through Lower Cretaceous fluvial strata of the Ghaggar-Hakra Formation. The
667 sedimentary succession includes channels, bars, sheet floods and overbank deposits in
668 varied proportions that typify a fluvial system deposited under subtropical climate
669 conditions. The immature, low sinuosity system of the Darjaniyon-ki Dhani Sandstone,
670 dominated by gravel bars and isolated channels, along with its frequently flooded and
671 poorly-drained floodplain, matures upward into the laterally migrating channel system of the
672 highly sinuous Sarnoo Sandstone. The Nosar Sandstone completes the formation at outcrop
673 and comprises stacked and amalgamated channels and gravel bars indicating fluvial
674 rejuvenation.

675 Fluvial rejuvenation is most likely a response to faulting and it is concluded tentatively that
676 the Nosar Sandstone may represent the onset or acceleration of rifting and development of
677 the eastern margin of the Barmer Basin. Consequently, the Nosar Sandstone, along with
678 contemporaneous and later sediments of the Ghaggar-Hakra Formation, is syn-rift in nature.
679 This conclusion supports that of Bladon et al. (2015a) derived from structural analysis and
680 provides further evidence that extension in the Barmer area of northwest India was probably
681 established prior to the start of the Palaeogene Period. Given this interpretation, well
682 developed successions of Cretaceous fluvial strata may be preserved in Mesozoic sections of
683 the subsurface of the WIRS, offering hydrocarbon potential below the presently explored
684 Palaeogene succession of the Barmer and related basins.

685 Early Cretaceous sediments are rarely exposed at outcrop across the northwest Indian Plate.
686 Comparisons between the Ghaggar-Hakra Formation and other successions of comparable
687 age, between their relative positions in a plate tectonic framework, and with regional
688 structural data, allow for a reconstruction of a detailed palaeogeographical map for this part
689 of the north-west Indian Plate for the early Cretaceous. The reconstruction suggests a more
690 complex fluvial drainage system than previously envisaged, with continental early
691 Cretaceous sediments preserved only within contemporaneous rifts.

692 **Acknowledgements**

693 This research was undertaken with matched funding from the Keele University Acorn Fund
694 and Cairn India Limited. Cairn India Limited also generously provided logistical support for all
695 fieldwork in Rajasthan for which the authors are very grateful. Bhanwar Lal, Andrew Bladon
696 and James Solan are thanked for their practical assistance and good humour in the field.

697 Colleagues within the Basin Dynamics Research Group at Keele and RPS Ichron are also
698 thanked for helpful discussions on sedimentology and basin analysis as our thoughts on the
699 Cretaceous of the Barmer Basin evolved. We extend our appreciation to the two referees
700 and journal editor Peter Swart for their valuable comments on the original manuscript.

701 We (the authors) have no conflict of interest to declare.

702 **References**

703 **Acharyya, S.K.** and **Lahiri, T.C.** 1991. Cretaceous palaeogeography of the Indian
704 subcontinent; a review. *Cretaceous Research*, 12, 3-26.

705 **Ahmad, A.H.M.** 1988. Facies analysis, sedimentation and diagenesis of Cretaceous
706 sandstones of north-eastern Gujarat. Aligarh Muslim University, PhD. Thesis.

707 **Ahmad, N.** and **Khan, M. R.** 2012 Evaluation of a distinct sub-play for enhanced exploration
708 in an emerging petroleum province, Bannu-Kohat sub-basin, Pakistan. *American*
709 *Association of Petroleum Geology, Search and Discovery Article 10391*, conference paper.

710 **Ahmad, N., Fink, P., Sturrock, S., Mahmood, T. and Ibrahim, M.** 2004. Sequence
711 Stratigraphy as Predictive Tool in Lower Goru Fairway, Lower and Middle Indus Platform,
712 Pakistan. Annual Technical Conference, ATC, 2004. 8-9 Oct., Islamabad.

713 **Ahmad, N., Fink, P., Sturrock, S., Mahmood, T. and Ibrahim, M.** 2012. Sequence
714 Stratigraphy as Predictive Tool in Lower Goru Fairway, Lower and Middle Indus Platform,
715 Pakistan. *AAPG Search and Discovery Article #10404*.

- 716 **Ahmad, R. and Amad, J.** 1991. Petroleum geology and prospects of the Sukkur Rift Zone,
717 Pakistan, with special reference to the Jaisalmer, Cambay and Bombay High basins of
718 India. *Pakistan Journal of Hydrocarbon Research*, 3(2), 33-41.
- 719 **Akhtar, K. and Ahmad, A.H.M.** 1991. Single-cycle cratonic quartzarenites produced by tropic
720 weathering: the Nimar sandstones (Lower Cretaceous), Narmada Basin, India.
721 *Sedimentary Geology*, 71, 23-32.
- 722 **Ali, J.R. and Aitchison, J.C.** 2014. Greater India's northern margin prior to its collision with
723 Asia. *Basin Research*, 26, 73-84.
- 724 **Aslam, M.** 1992. Delta plain coal deposits from the Than Formation of the Early Cretaceous
725 Saurashtra Basin, Gujarat, western India. *Sedimentary Geology*, 81, 181-193.
- 726 **Baksi, S.K. and Naskar, P.** 1981. Fossil Plants from the Sarnu Hill Formation, Barmer Basin,
727 Rajasthan, *The Palaeobotanist*, 27, 107-111.
- 728 **Balakrishnan, T.S., Unnikrishnan, P. and Murty, A.V.S.** 2009. The Tectonic Map of India and
729 Contiguous Areas. *Journal of the Geological Society of India*, 74, 158-170.
- 730 **Banham, S.G. and Mountney, N.P.** 2013. Climatic versus halokinetic control on
731 sedimentation in a dryland fluvial succession: Triassic Moenkopi Formation, Utah, USA.
732 *Sedimentology*, 61, 570-608.

- 733 **Bastia, R., Reeves, C., Pundarika, Rao D., D'Silva K. and Radhakrishna M.** 2010.
734 Paleogeographic reconstruction of east gondwana and evolution of the Indian Continental
735 margin. DCS-DST News, 2-8.
- 736 **Basu, A.R., Renne, P.R., DasGupta, D.K., Teichman, F. and Poreda, R.J.** 1993. Early and late
737 alkali igneous pulses and a high ³He plume origin for the Deccan Flood basalts. Science
738 261, 902-906.
- 739 **Best, J.L., Ashworth, P.J., Bristow, C.S. and Roden, J.** 2003. Three-dimensional sedimentary
740 architecture of a large, mid-channel sand braid bar, Jamuna River, Bangladesh. Journal of
741 Sedimentary Research, 73, 516-530.
- 742 **Bhatt, N.Y., Solanki, P.M., Prakash, N. and Das, N.** 2016. Depositional environment of
743 Himmantnagar Sandstone (Lower/Middle Cretaceous): a perspective, The Palaeobotanist,
744 56, 67-84.
- 745 **Biswas, S.K.** 1982. Rift Basins in Western Margin of India and Their Hydrocarbon Prospects
746 with Special Reference to Kutch Basin. American Association of Petroleum Geology
747 Bulletin, 66, 1497-1513.
- 748 **Biswas, S.K.** 1987. Regional tectonic framework, structure and evolution of the western
749 marginal basins of India. Tectonophysics, 135, 307-327.

- 750 **Biswas, S.K.** 1999. A review on the evolution of rift basins in India during Gondwana with
751 special reference to the western Indian basins and the hydrocarbon prospects. PINAS, 3,
752 261-283.
- 753 **Bladon, A.J., Burley, S.D., Clarke, S.M. and Beaumont, H.** 2015a. Geology and regional
754 significance of the Sarnoo Hills, eastern rift margin of the Barmer Basin, northwest India.
755 Basin Research, 27, 636-655.
- 756 **Bladon, A.J., Clarke, S.M. and Burley S.D.** 2105b. Complex rift geometries resulting from
757 inheritance of pre-existing structures: Insights and regional implications from the Barmer
758 Basin rift, Journal of Structural Geology, 71, 136-154.
- 759 **Blair, T.C.** 2000. Sedimentary and progressive tectonic unconformities of the sheet flood-
760 dominated Hell's Gate alluvial fan, Death Valley, California. Sedimentary Geology, 132,
761 233-262.
- 762 **Blair, T.C. and McPherson, J.G.** 1994. Alluvial fans and their natural distinctions from rivers
763 based on morphology, hydraulic processes, sediment processes and facies assemblages,
764 Journal of Sedimentary Research, A64, 450-489.
- 765 **Bordy, E.M., Hancox, P.J. and Rubidge, B.S.** 2004. Fluvial style variations in the Late Triassic-
766 Early Jurassic Elliot Formations, main Karoo Basin, South Africa, Journal of African Earth
767 Sciences, 38, 383-400.

768 **Bridge, J.S.** 1993. The interaction between channel geometry, water flow, sediment
769 transport and deposition in braided rivers. Geological Society London, Special Publication,
770 75, 13-71.

771 **Bridge, J.S., Alexander, J., Collier, R.E.L.L., Gawthorpe, R.L. and Jarvis, J.** 1995. Ground-
772 penetrating radar and coring used to study the large-scale structure of point-bar deposits
773 in three dimensions. *Sedimentology*, 42, 839-852.

774 **Bridge, J.S. and Best, J.L.** 1988. Flow, sediment transport and bedform dynamics over the
775 transition from dunes to upper-stage plane beds: implications for the formation of planar
776 laminae. *Sedimentology*, 35, 753-763.

777 **Bridge, J.S. and Leeder, M.R.** 1979. A simulation of model alluvial stratigraphy.
778 *Sedimentology*, 26, 617-644.

779 **Brierley, G., Fergusin, R.J. and Woolfe, K.J.** 1997. What is a fluvial levee? *Sedimentary*
780 *Geology*, 114, 1-9.

781 **Bromley, R.G. and Asgaard, U.** 1979. Triassic freshwater ichnocoenoses from Carlsberg
782 Fjord, East Greenland. *Palaeogeography, Palaeoclimate, Palaeocology* 28, 39-80.

783 **Bromley, R.G. and Asgaard, U.** 1991. Ichnofacies: a mixtrure of taphofacies and biofacies.
784 *Lethaia*, 24, 153-163.

- 785 **Buatois, L.A. and Mangano, M.G.** 2002. Trace fossils from Carboniferous floodplain deposits
786 in Western Argentina: implications for ichnofacies models of continental environments.
787 *Palaeogeography, Palaeoclimate and Palaeoecology*, 183, 71-86.
- 788 **Cant, D.J. and Walker, R.G.** 1978. Fluvial processes and facies sequences in the sandy South
789 Saskatchewan River, Canada. *Sedimentology*, 25, 625-648.
- 790 **Casshyap, S.M. and Aslam, M.** 1992. Deltaic and shoreline sedimentation in Saurashtra
791 Basin, western India: An example of infilling in an early Cretaceous failed rift. *Journal of*
792 *Sedimentary Petrology*, 62, 972-991.
- 793 **Cecil, C.B. and Dulong, F.T.** 2013. Precipitation models for sediment supply in warm
794 climates. *Climate Controls on Stratigraphy*, SEPM Special Publication No. 77, 21-27.
- 795 **Chatterjee, S., Goswami, A. and Scotese, C.R.** 2013. The longest voyage: Tectonic,
796 magmatic, and paleoclimatic evolution of the Indian plate during its northward flight from
797 Gondwana to Asia. *Gondwana Research*, 23, 238-267.
- 798 **Chowdhary, L.R.** 1975. Reversal of basement-block motions in Cambay Basin, India, and its
799 importance in petroleum exploration. *American Association of Petroleum Geologists*
800 *Bulletin*, 59, 85-96.
- 801 **Collier, J.S., Sansom, V., Ishizuka, O., Taylor, R.N., Minshull, T.A. and Whitmarsh, R.B.** 2008.
802 Age of Seychelles-India break-up. *Earth and Planetary Sciences Letters*, 272, 264-277.

- 803 **Compton, P.M.** 2009. The geology of the Barmer Basin, Rajasthan, India and the origins of its
804 major oil reservoir, the Fatehgarh Formation. *Petroleum Geoscience*, 15, 117-130.
- 805 **Crawford, A.R.** and **Compton, W.** 1969. The age of the Vindhyan System of Peninsular India.
806 *Quarterly Journal of the Geological Society*, 125, 351-371.
- 807 **Dasgupta, S.** and **Mukherjee, S.** 2017. Brittle shear tectonics in a narrow continental rift:
808 asymmetric non-volcanic Barmer Basin (Rajasthan, India). *The Journal of Geology*, 125,
809 561-591.
- 810 **Desai, A.G.** and **Desai, S.J.** 1989. Himatnagar Sandstones of north Gujarat their depositional
811 environment and tectonic framework, Ph.D. Thesis, Maharaja Sayajirao University of
812 Baroda.
- 813 **Dev, S.** 1987. Floristic zones in the Mesozoic formations and their relative age.
814 *Palaeobotanist*, 36, 161-167
- 815 **Dolson J., Burley S.D., Sunder, V.R., Kothari, V., Naidu B., Whiteley, N.P., Farrimond, P.,**
816 **Taylor, A., Direen, N.** and **Ananthkrishnan, B.** 2015. The discovery of the Barmer Basin,
817 Rajasthan, India and its petroleum geology. *American Association of Petroleum Geology*
818 *Bulletin*, 99, 433-465.
- 819 **Eagles, G.** and **Hoang, H.H.** 2014. Cretaceous to present kinematics of the Indian, African and
820 Seychelles plates. *Geophysical Journal International*, 196, 1-14.

- 821 **Fielding, C.R., Allen, J.P., Alexander, J. and Gibling, M.R.** 2009. Facies model for fluvial
822 systems in the seasonal tropics and subtropics. *Geological Society of America*, 37, 623-626.
- 823 **Froude, M.J., Alexander, J., Barclay, J. and Cole, P.** 2017. Interpreting flash flood palaeoflow
824 parameters from anti-dunes and gravel lenses: An example from Montserrat, West Indies.
825 *Sedimentology*, 64, 1817-1845.
- 826 **Ganerød, M., Torsvik, T.H., van Hinsbergen, D.J.J., Gaina, C., Corfu, F., Werner, S., Owen-**
827 **Smith, T.M., Ashwal, L.D., Webb S.J. and Hendriks B.W.H.** 2011. Palaeoposition of the
828 Seychelles microcontinent in relation to the Deccan Traps and the Plume Generation Zone
829 in the late Cretaceous-early Palaeogene time. *Geological Society of London, Special*
830 *Publications*, 357, 229-252.
- 831 **Gawthorpe, R.L. and Leeder, M.R.** 2000. Tectono-sedimentary evolution of active
832 extensional basins. *Basin Research* 12, 195-218.
- 833 **Ghazi, S. and Mountney N.P.** 2009. Facies and architectural element analysis of a
834 meandering fluvial succession: The Permian Warchha Sandstone, Salt Range, Pakistan.
835 *Sedimentary Geology* 221, 99-126.
- 836 **Ghinassi, M.** 2010. Chute channels in the Holocene high-sinuosity river deposits of the
837 Firenze plain, Tuscany, Italy. *Sedimentology* 58, 618-642.
- 838 **Goswami, A.** 2011. Predicting the geographic distribution of ancient soils with special
839 reference to the Cretaceous. Ph.D. Thesis, University of Texas, Arlington, Texas.

840 **Gowland, S., Taylor, A.M. and Martinius A.W.** 2018. Integrated sedimentology and
841 ichnology of Late Jurassic fluvial point-bars – facies architecture and colonization styles
842 (Lourinha Formation, Lusitanian Basin, western Portugal). *Sedimentology*, 65, 400-430.

843 **Grotzinger, J.P., Arvidson, R.E., Bell, III, J.F., Calvin, W., Clark, B.C., Fike, D.A., Golombek,**
844 **M., Greeley, R., Haldermann, A., Herkenhoff, K.E., Jolliff, B.L., Knoll, A.H., Malin, M.,**
845 **McLennan, S.M., Parker, T., Soderblom, L., Sohl-Dickstein, J.N., Squyres, S.W., Tosca,**
846 **N.J. and Watters W.A.,** 2005. Stratigraphy and sedimentology of a dry and wet eolian
847 depositional system, Burns Formation, Meridiani Planum, Mars. *Earth and Planetary*
848 *Science Letters* 240, 11-72.

849 **Gulliford, A.R., Flint S.S. and Hodgson D.M.** 2014. Testing applicability of models of
850 distributive fluvial systems or trunk rivers in ephemeral systems: reconstructing 3-D
851 fluvial architecture in the Beaufort Group, South Africa. *Journal of Sedimentary Research*
852 84, 1147-1169.

853 **Hallam, A.** 1985. A review of Mesozoic climates. *Journal of Geological Society of London* 142,
854 433-445.

855 **Hampton, B.A. and Horton, B.K.** 2007. Sheetflood fluvial processes in a rapidly subsiding
856 basin, Altiplano plateau, Bolivia, *Sedimentology* 54, 1121-1147.

857 **Hjellbakk, A.** 1997. Facies and fluvial architecture of a high-energy braided river: the upper
858 Proterozoic Segloddan Member, Varanger Peninsula, northern Norway. *Sedimentary*
859 *Geology* 114, 131-161.

- 860 **Hunter, R.E.** 1977a. Terminology of cross-stratified sedimentary layers and climbing-ripple
861 structures. *Journal of Sedimentary Petrology* 47, 697-706.
- 862 **Hunter, R.E.** 1977b. Basic types of stratification in small eolian dunes. *Sedimentology* 24,
863 361-387.
- 864 **Ielpi, A.** and **Ghinassi, M.** 2014. Planform architecture, stratigraphic signature and
865 morphodynamics of an exhumed Jurassic meander plain (Scalby Formation, Yorkshire,
866 UK). *Sedimentology* 61, 1923-1960.
- 867 **Jackson, R.G.** 1976. Depositional model of point bars in the lower Wabash River, *Journal of*
868 *Sedimentary Petrology*, 46, 579 – 594.
- 869 **Jaitly, A.K.** and **Ajane, R.** 2013. Comments on *Placenticerias Mintoii* (Vredenburg, 1906) from
870 the Bagh Beds (Late Cretaceous), Central India with Special Reference to Turonian
871 Nodular Limestone Horizon. *Journal of the Geological Society of India*, 81, 565-574.
- 872 **Jana, B.N., King, S.C.** and **Hilton, J.** 2013. Revision of the Cretaceous fossil plant-assemblage
873 from Gardeshwar (Gujarat, India): A conifer dominated floral associations from an Upper
874 Gondwana sequence on the West Coast of India. *Journal of Asian Earth Sciences*, 73, 128-
875 138
- 876 **Jones, B.G.** and **Rust, B.R.** 1982. Massive sandstone facies in the Hawkesbury Sandstone, a
877 Triassic fluvial deposit near Sydney, Australia. *Journal of Sedimentology Petrology* 54(4),
878 1249-1259.

- 879 **Khalid, P., Qayyum, F. and Yasin, Q.** 2014. Data-driven sequence stratigraphy of the
880 Cretaceous depositional system, Punjab Platform, Pakistan. *Survey Geophysics*, 35, 1065-
881 1088.
- 882 **Khosla, A., Kapur, V.V., Sereno, P.C., Wilson, J.A., Wilson, G.P., Dutheil, D., Sahnj, A., Singh,**
883 **M.P., Kumar, S. and Rana, R.S.** 2003. First Dinosaur remains from the Cenomanian
884 Turonian Nimar Sandstone (Bagh Beds), District Dhar, Madhya Pradesh, India. *Journal of*
885 *the Palaeontological Society of India*, 48, 115-127.
- 886 **Kothari, V., Naidu, B., Sunder, V.R., Dolson, J., Surley, S.D., Whiteley, N.P., Mohapatra, P.**
887 **and Ananthkrishnan, B.,** 2015. Discovery and petroleum system of Barmer Basin, India.
888 (abs.): American Association of Petroleum Geology, Search and discovery article #110202,
889 conference paper.
- 890 **Kraus, M.J.** 1999. Paleosols in clastic sedimentary rocks: their geologic applications. *Earth*
891 *Science Reviews* 47, 41-70.
- 892 **Kraus, M.J. and Aslan, A. 1999.** Palaeosol sequences in floodplain environments: a
893 hierarchical approach. *Special Publications International Association of Sedimentologists*,
894 27, 303-321
- 895 **Kraus, M.J. and Hasiotis, S.T.** 2006. Significance of different modes of rhizolith preservation
896 to interpreting paleoenvironmental and paleohydrologic settings: examples from
897 Paleogene palaeosols, Bighorn Basin, Wyoming, USA. *Journal of Sedimentary Research*,
898 76, 633-646.

- 899 **Leeder, M.R.** 1993. Tectonic controls upon drainage basin development, river channel
900 migration and alluvial architecture: implications for hydrocarbon reservoir development
901 and characterization. Geological Society, London, Special Publications 73, 7-22.
- 902 **Lowe, D.R.** 1988. Suspended-load fallout rate as an independent variable in the analysis of
903 current structures. *Sedimentology* 35, 765-776.
- 904 **Martin, C.A.L. and Turner, B.R.** 1998. Origins of massive-type sandstones in braided river
905 systems. *Earth-Science Reviews* 44, 15-38.
- 906 **Mather, A., Stokes, M., Pirrie, D. and Hartley, R.** 2008. Generation, transport and
907 preservation of armoured mudballs in an ephemeral gully system. *Geomorphology* 100,
908 104-119.
- 909 **Miall, A.D.** 1985. Architectural-Element Analysis: A New Method of Facies Analysis Applied
910 to Fluvial Deposits. *Earth Science Review* 22, 261-308.
- 911 **Miall, A.D.** 1988. Architectural elements and bounding surfaces in fluvial deposits: anatomy
912 of the Kayenta Formation (Lower Jurassic), southwest Colorado. *Sedimentary Geology* 55,
913 233-262.
- 914 **Mishra, P.C., Singh N.P., Sharma D.C., Kakaroo A.K., Upadhyay, H. and Saini, M.L.** 1993.
915 Lithostratigraphy of Indian Petroliferous Basins, Document II. West Rajasthan Basins,
916 KDMIPE, ONGC Publication: 1-123.

- 917 **Misra, A.A. and Mukherjee, S.** (2015) Tectonic Inheritance in Continental Rifts and Passive
918 Margins. Springerbriefs in Earth Sciences. ISBN 978-3-319-20576-2.
- 919 **Mohan, M.** (1995) Cambay Basin – A promise of oil and gas potential. Journal of The
920 Palaeontological Society of India, 40, 41 – 47.
- 921 **Morgan, W.J.** 1971. Convection plumes in the lower mantle. Nature 23, 42-43.
- 922 **Mukherjee, M.K.** 1983. Petroleum prospects of Cretaceous sediments of the Cambay Basin,
923 Gujarat, India. Journal of Petroleum Geology 5, 275-286.
- 924 **Mukherjee, S., Misra, A.A., Calvès, G., and Nemčok, M.** 2017. Tectonics of the Deccan Large
925 Igneous Province: an introduction. In: **Mukherjee S, Misra AA, Calvès G, Nemčok M.** (Eds)
926 Tectonics of the Deccan Large Igneous Province. Geological Society, London, Special
927 Publications 445, 1-9.
- 928 **Najman, Y., Burley, S.D., Copley, A.C., Kelly, M.J., Pandey, K. and Mishra, P.** 2018. The
929 Oligocene unconformity of the Himalayan and NW Indian intraplate basins: a record of
930 tectonics or mantle dynamics. Tectonics, Manuscript in review.
- 931 **O’Conner, J.E., Jones, M.A. and Haluska, T.L.** 2003. Flood plain and channel dynamics of the
932 Quinault and Queets Rivers, Washington, USA. Geomorphology, 51, 31-59

- 933 **Pandey, D.K., Fursich, F.T. and Sha, J-G.** 2009. Interbasinal marker intervals – A case study
934 from the Jurassic basins of Kachchh and Jaisalmer, western India. Science in China Press,
935 52, 1924-1931.
- 936 **Plummer, P.S. and Belle, E.R.** 1995. Mesozoic tectono-stratigraphic evolution of the
937 Seychelles microcontinent. Sedimentary Geology, 96, 73-91.
- 938 **Plummer, P.S., Joseph, P.R. and Samson, P.J.** 1998. Depositional environments and oil
939 potential of Jurassic/Cretaceous source rocks within the Seychelles microcontinent.
940 Marine and Petroleum Geology, 15, 385-401.
- 941 **Posmentier, H.E. and Kolla, V.** 2003. Seismic geomorphology and stratigraphy of
942 depositional elements in deep-water settings. Journal of Sedimentary Research, 73, 367-
943 388.
- 944 **Racey, A., Fisher, J., Bailey, H. and Kumar-Roy, S.** 2016. The value of fieldwork in making
945 connections between onshore outcrops and offshore models: an example from India.
946 Geological Society of London, Special Publications, 436, 21-53.
- 947 **Rai, J., Singh, A. and Pandey, D.K.** 2013. Early to middle Albian age calcareous nannofossils
948 from Pariwar Formation of Jaisalmer Basin, Rajasthan, western India and their
949 significance. Current Science, 105, 1604-1611.
- 950 **Rajanikath, A. and Chinnappa, C.H.** 2016. Early Cretaceous flora of India—A review. The
951 Palaeobotanist, 65, 209-245.

- 952 **Rajaram, M., Anand, S.P., Erram, V.C. and Shinde, B.N.** 2016. Insight into the structures
953 below the Deccan Trap-covered region of Maharashtra, India from geopotential data.
954 Geological Society of London, 445, 219-236
- 955 **Raju, A.T.R.** 1968. Geological evolution of Assam and Cambay Tertiary Basins of India.
956 American Association of Petroleum Geology Bulletin, 52, 2422-2437.
- 957 **Rao, K.M., Kumar, M.R. and Rastogi, B.K.** 2015. Crust beneath the northwestern Deccan
958 Volcanic Province India: Evidence for uplift and magmatic underplating. Journal of
959 Geophysical Research Solid Earth, 120(5), 3385-3405.
- 960 **Reeves, C.** 2014. The position of Madagascar within Gondwana and its movements during
961 Gondwana dispersal. Journal of African Earth Sciences, 94, 45-57.
- 962 **Reeves, C. and De-Wit, M.** 2000. Making ends meet in Gondwana: retracing the transforms
963 of the Indian Ocean and reconnecting continental shear zones. Terra Nova, 12, 272-280.
- 964 **Retallack, G.J.** 1988. Field recognition of paleosols, Geological Society of America Special
965 Papers, 216, 1-20.
- 966 **Retallack, G.J.** 1990. Soils of the Past: An introduction to paleopedology. Harper Collins
967 Academic, Hammersmith.
- 968 **Robinson, J.W. and McCabe, P.J.** 2012. Evolution of a braided river system: the Salt Wash
969 Member of the Morrison Formation (Jurassic) in southern Utah. Society of Sedimentary
970 Geology, special publication, 59, 93-107.

- 971 **Roy, A.B. and Jokhar, S.R.** 2002. Geology of Rajasthan (Northwest India) Precambrian to
972 recent, Pawan Kumar. Scientific Publishers, India. Jodhpur, India.
- 973 **Schumm, S.A.** 1981. Evolution and response of the fluvial system, sedimentologic
974 implications. The Society of Economic Paleontologists and Mineralogists, Special
975 Publications, 31, 19-29.
- 976 **Schumm, S.A.** 1993. River Response to Baselevel Change: Implications for Sequence
977 Stratigraphy. Journal of Geology, 101, 279-294.
- 978 **Scotese, C.R.** 2011. The PALEOMAP Project paleoatlas for ArcGIS, volume 2, Cretaceous
979 paleogeographic and plate tectonic reconstructions. PALEOMAP Project, Arlington, Texas.
- 980 **Scotese, C.R., Illich, H., Zumberge, J. and Brown, S.** 2007. The GANDOLPH Project: One-year
981 report: Paleogeographic and palaeoclimate controls on hydrocarbon source rock
982 deposition, A report on the methods employed, the results of the paleoclimate
983 simulations (FOAM) and oil/source rock compilation for the late Cretaceous
984 (Cenomanian/Turonian; 93.5 Ma), late Jurassic (Kimmeridgian/Tithonian; 151 Ma), Early
985 Permian (Sakmarin/Artinskian; 248 Ma) and late Devonian (Frasnian/Femennian; 372
986 Ma), Conclusions at the end of year one. GeoMark Research LTD, Houston, Texas.
- 987 **Sharma, K.K.** 2007. K-T magmatism and basin tectonism in western Rajasthan, India: results
988 from extensional tectonics and not from Reunion plume activity. In: Foulger, G.R., and
989 Jurdy, D.M., (Eds.). Plates, Plumes and Planetary Processes. Geological Society of America
990 Special Paper, 430, 775-784.

- 991 **Sheth, H.C.** 2007. Large Igneous Provinces (LIPs): Definition, recommended terminology and
992 a hierarchical classification. *Earth Science Reviews*, 85, 117-124.
- 993 **Simonetti, A., Bell K. and Viladkar, S.G.** 1995. Isotopic data from the Amba Dongar
994 carbonatite complex, west-central India: evidence for an enriched mantle source.
995 *Chemical Geology*, 122, 185-198.
- 996 **Singh, N.P.** 2006. Mesozoic lithostratigraphy of the Jaisalmer Basin, Rajasthan. *Journal of the*
997 *Palaeontological Society of India*, 51(2), 1 – 25.
- 998 **Sisodia, M.S. and Singh, U.K.** 2000. Depositional environment and hydrocarbon prospects of
999 the Barmer Basin, Rajasthan, India. *North American Free Trade Association*, 9, 309-326.
- 1000 **Smewing, J.D., Warburton, J., Daley, T., Copestake, P. and Ul-haq, N.** 2002. Sequence
1001 stratigraphy of the southern Kirthar Fold Belt and Middle Indus Basin, Pakistan: In: Clift,
1002 P.D., Gaedicke, D., Craig, J., (eds). *The tectonics and climatic evolution of the Arabian Sea*
1003 *Regions; geological Society, London, Special Publications*, 195, 273-299.
- 1004 **Storey, M., Mahoney, J.J., Saunders, A.D., Duncan R.A., Kelley, S.P. and Coffin, M.F.** 1995.
1005 Timing of hot-spot related volcanism and the break-up and Madagascar and India.
1006 *Science*, 267, 852-855
- 1007 **Tabaei, M. and Singh, R.Y.** 2002. Paleoenvironment and paleoecological significance of
1008 microforaminiferal linings in the Akli Lignite, Barmer Basin, Rajasthan, India. *Iranian*
1009 *International Journal of Science*, 3, 263-277.

- 1010 **Tennvassås, I.** 2018. Characterisation of palaeosols in the Lower Cretaceous Helvetiafjellet
1011 Formation, Svalbard. The University of Norway, Master Thesis.
- 1012 **Torsvik, T.H., Amundsen, H., Hartz, E.H., Corfu, C., Kuznir, N., Gaina, C., Doubrovine, P.V.,**
1013 **Steinburger, B., Ashwal, L.D. and Jamtveit, B.** 2013. A Precambrian microcontinent in the
1014 Indian Ocean. *Nature Geoscience*, 6, 223-227.
- 1015 **Torsvik, T.H., Tucker, R.D., Ashwal, L.D., Carter, L.M., Jamtveit, B., Vidyadharan, T. and**
1016 **Venkataramana, P.** 2000. Late Cretaceous India-Madagascar fit and timing of break-up
1017 and related magmatism. *Terra Nova*, 12, 220-225.
- 1018 **Tripathi, S.K.M., Kumar, M. and Srivastava, D.** 2009. Palynology of Lower Palaeogene
1019 (Thanetian-Ypresian) coastal deposits from the Barmer Basin (Akli Formation, Western
1020 Rajasthan, India): Palaeoenvironmental and palaeoclimatic implications. *Geological Acta*,
1021 7, 147-160.
- 1022 **Wakefield, O.J.W., Hough, E. and Peatfield, A.W.** 2015. Architectural analysis of a Triassic
1023 fluvial system: The Sherwood Sandstone of the East Midlands Shelf, UK. *Sedimentary*
1024 *Geology*, 327, 1-13.
- 1025 **Wilson, A.A.** 1993. The Merica Mudstone Group (Trias) of the Cheshire Basin, *Proceedings of*
1026 *the Yorkshire Geological Society*, 49, 171-188.




1027 **Zaigham, N.A. Ahmad, M. and Hisam, N.** 2012. Thar Rift and its significance for
1028 hydrocarbons. American Association of Petroleum Geology Search and Discovery Article,
1029 2014, conference paper.

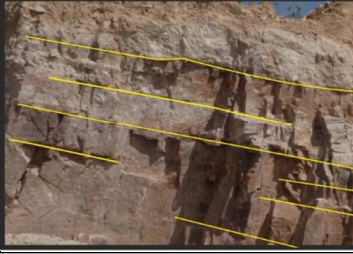




1030 **Zaigham, N.A. and Mallick, K.A.** 2000. Prospect of hydrocarbon associated with fossil-rift
1031 structures of the southern Indus basin, Pakistan. American Association of Petroleum
1032 Geology Bulletin, 84, 1833-1848.




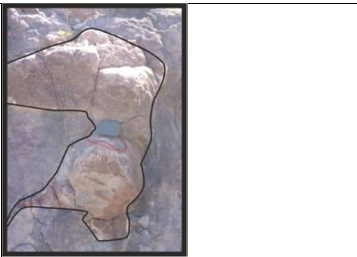
1033 **Table captions**

1034 Table 1: Fluid, debris and subaerial facies of the Ghaggar-Hakra Formation developed from
1035 the logged and panelled data of the formation.

1036 Table 2: Architectural elements of the Ghaggar-Hakra Formation.

Lithofacies	Texture	Structures	Interpretation	GPS Location	Figure
Fluid flow facies					
G (clast supported conglomerate)	Sub-rounded pebble-grade quartz and lithic clasts (2 – 52 mm), poorly sorted.	Erosional surfaces, grading of the clasts and indistinct cross-beds	Confined lower flow regime, potential migration of dune-scale bedforms	UTM 0777247, 2841083	
Stx (Trough cross-bedded sandstone)	Fine- to coarse-grained sands, moderately sorted, sub-rounded with rounded pebbles of quartz (22 mm)	Trough cross-bedding and erosional surfaces	Migration of sinuous crested dune-scale bedforms in the lower-flow regime	UTM 0778735, 2842021	
Sx (Planar cross-bedded sandstone)	Fine- to coarse-grained, well sorted, sub-rounded, with rounded pebbles of quartz (50 mm)	Planar cross-bedding, u-shape structures, reactivation and erosional surfaces	Migration of straight crested dune-scale bedforms in the lower-flow regime	UTM 0782621, 2853326	

Sb (Parallel bedded sandstone)	Very fine- to coarse-grained, moderately sorted, sub-rounded, clasts (22 mm).	Parallel bedding, erosional surfaces, silt bands, with very occasional cross-beds.	Non- or partially-confined flow events with bedload dominant transport and sporadic dune bedforms	UTM 0782621, 2853326	
Sla (Low-angle cross-bedded sandstone)	Fine- to coarse-grained sands, moderately sorted, sub-rounded	Low angle cross-bedding	Sediments likely deposited due to helical flow during lateral migration	UTM 0777898, 2840794	
Sr (Rippled sandstone)	Very fine- to medium-grained, well sorted, sub-rounded	Symmetrical and asymmetrical ripples upon laminated and bedded sediments	Ripple-scale bedforms in the lower flow regime	UTM 0777801, 2841812	
Srha (Rippled sandstone with supercritical climbing)	Very fine- to medium-grained, well sorted, sub-rounded	Fully preserved symmetrical and asymmetrical ripples	Ripple-scale bedforms in the lower flow regime; high sediment output	UTM 0783859, 2853121	
Scl (Cross-lamination sandstone)	Fine-grained sands, well sorted, sub-angular	Cross-lamination	Ripple-scale bedforms in the lower-flow regime	UTM 0783859, 2853121	

<p>Sh (Horizontally-laminated)</p>	<p>Fine- to medium-grained sands, moderately sorted, sub-angular</p>	<p>Laminations</p>	<p>Low amplitude, long wavelength bedforms of the upper flow regime</p>	<p>UTM 0783727, 2853017</p>	
<p>Sm (Massive sandstone)</p>	<p>Fine- to coarse-grained, on occasion there are clasts up to 19 mm.</p>	<p>Massive</p>	<p>Material deposition from suspension, in very low slow moving or stationary waters</p>	<p>UTM 0777107, 2840577</p>	
<p>Im (Massive siltstone)</p>	<p>Siltstone</p>	<p>Massive</p>	<p>Material deposition from suspension, in stationary waters</p>	<p>UTM 0777181, 2841039</p>	
<p>Debris flow facies</p>					
<p>M (Matrix-supported conglomerate)</p>	<p><27 cm boulders, where the matrix is granule-grade conglomerates; the material is matrix-supported</p>	<p>Indistinct cross-bedding</p>	<p>Non-Newtonian flow resulting from high sediment load suppression of bedforms</p>	<p>UTM 0777865, 2841891</p>	
<p>Subaerial facies</p>					


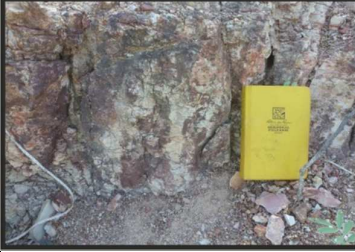

Sp (Pedogenic sandstone)	Mottled red and white very fine-grained sands	Occasional laminations, soft sediment deformation and indistinct bedding and laminations	Bioturbation from plants and organisms and a pedogenic nature equalling soil formation	UTM 0778635, 2842386	
Ip (Pedogenic siltstone)	Mottled red and white, muds and silts	Occasional laminations, soft sediment deformation and indistinct bedding and laminations	Pedogenic nature, soil slickenlines, fractures and bioturbation from root traces and organisms allowing for soil formation	UTM 0778640, 2842381	
Ihe (Haematitic siltstone)	Mottled red and white, muds and silts	Haematitic horizons with occasional laminations, soft sediment deformation and indistinct bedding and laminations	Bioturbation from plants and organisms, haematitic and a pedogenic nature equalling soil formation	UTM 0778635, 2842386	

Table 1

AE	Litho-facies	Description	Interpretation
Ch	G, Stx, Sx, Scl, Sh, Sp	<p><u>Geometry:</u> Tabular and sheet-like geometries</p> <p><u>Size:</u> up to 6 m thick</p> <p><u>External boundaries:</u> Lower fifth order surfaces are erosional and the upper fourth boundaries are gradational where seen</p>	Packages of sediment represent in-channel deposits.

		<u>Internal boundaries:</u> First to third order bounding surfaces	
Cm	Sx, Sh, Scl, Sp, Ip	<u>Geometry:</u> Wedged and tabular <u>Size:</u> Up to 5 m thick and 10 wide <u>External boundaries:</u> Lower fifth order surface is sharp and the upper fourth order surface is gradational. <u>Internal boundaries:</u> First to third order bounding surfaces	Deposited due to flow migrating from a confined to an unconfined setting.
Gb	G, M, Sm, Sh	<u>Geometry:</u> Lenticular to wedge shaped <u>Size:</u> <6 m high and 300 m in lateral extension <u>External boundaries:</u> Lower fifth order boundaries are erosion and the upper fourth order boundaries are gradational. <u>Internal boundaries:</u> First to third order surfaces	Transient braid bars, with deposition by migrating bedforms.
Cc	G, Sm, Im, Sh, Sp, Ip	<u>Geometry:</u> Lenticular and wedged shaped <u>Size:</u> Channels are <70 cm in height and 2 m wide <u>External boundaries:</u> Lower fifth order boundaries are erosional and the upper fourth order boundaries are gradational <u>Internal boundaries:</u> No internal bounding surfaces, generally structureless, can contain normal grading	Flooding of the river system by cutting off the point bar.
Pb	Sla, Sx, Scl	<u>Geometry:</u> Wedge <u>Size:</u> <3 m in height, and 20 m in length <u>External boundaries:</u> Lower order fifth order bounding surface and the fourth order bounding surface are gradational <u>Internal boundaries:</u> First and second order bounding surface which truncate against third and fourth order bounding surfaces where the sets and cosets are perpendicular to one another	Laterally migrating bars
Sf	Sr, Sh, Srha, Sb, Scl, Sp, Ip	<u>Geometry:</u> Sheet-like and tabular <u>Size:</u> laterally extensive (< 2 km) and 2 m high <u>External boundaries:</u> Lower fifth order bounding surface is concave-down and concordant and the upper fourth order bounding surface is gradational <u>Internal boundaries:</u> Interbedded laminations and ripples with first and second order bounding surfaces	Formed through the flooding of the fluvial system.
Ob	Sh, Sm, Im, Sr, Scl,	<u>Geometry:</u> Tabular and sheet-like <u>Size:</u> up to 150 cm in thickness and 2 km in lateral extension <u>External boundaries:</u> Lower sixth order bounding surface is sharp and the upper fourth order bounding surface is sharp	Formed from cyclic flooding from the fluvial system, with palaeosol evident.

	Sp, Ip, Ihe	<u>Internal boundaries:</u> First to fifth order surfaces are present; the first to third order surfaces are from ripples, fourth order surfaces are sharp and form from the pond element. The fifth order surfaces are regional quiescence periods.	
Po	Scl, Sm, Im, Sr, Sh, Ip, Ihe	<u>Geometry:</u> Sheet-like and tabular <u>Size:</u> <0.5 m high and 20 m in length <u>External boundaries:</u> both the lower and upper fourth order boundaries are gradational into the floodplain element <u>Internal boundaries:</u> First and second order surfaces present with boundaries removed due to bioturbation.	Slight coarsening upwards successions, capped with palaeosols.

Table 2

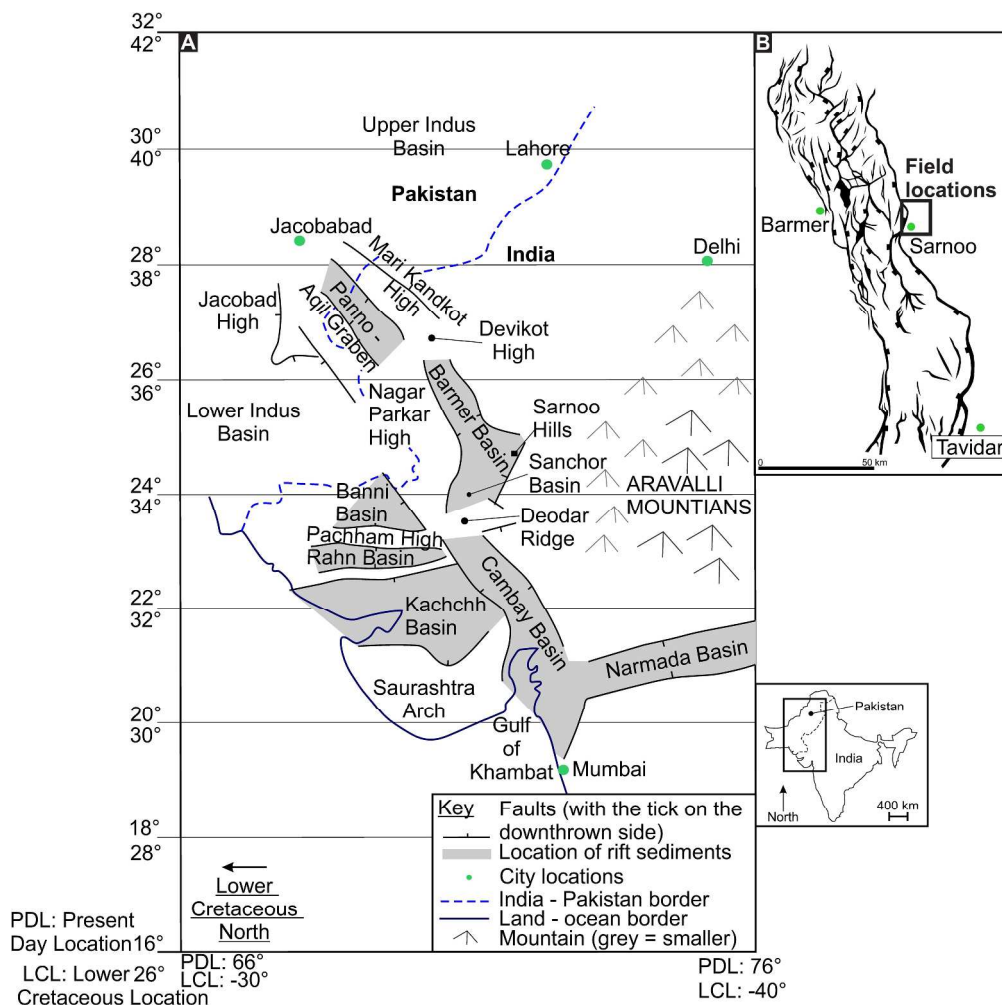


Figure 1: (A) Onshore rift basins within the WIRS (adapted from Balakrishnan et al., 2009) and various locations mentioned in the text: Insert gives the location of the Barmer Basin indicated by the solid black line within the Barmer District; (B) Principal extensional faults that define the geometry and limits of the Barmer Basin (adapted from Dolson et al., 2015), displaying the field locations for this study on the eastern, central margin. The settlement of Sarnoo is shown.

301x299mm (300 x 300 DPI)

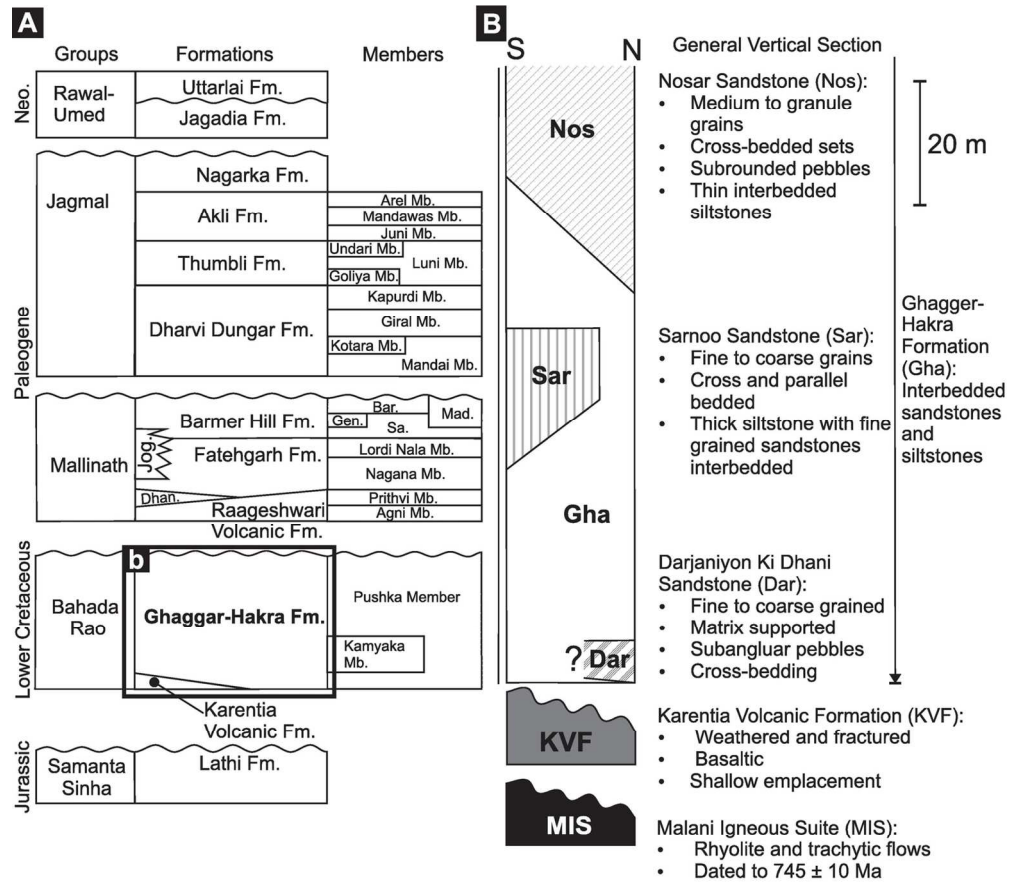


Figure 2: (A) Generalised vertical section of the Barmer Basin, displaying currently accepted group formations and members; Dhan. = Dhandlawas Formation, Jog. = Jogmaya Mandir Formation, Sa. = Sarovar Member, Gen. = Genhu hill Member, Mad. = Madpura Member, Bar. = Bariyada Member (Compton, 2009; Dolson et al., 2015; Sisodia & Singh, 2000; Tabaei & Singh, 2002; Tripath et al., 2009); (B) generalised vertical section of the Ghaggar-Hakra Formation, displaying the separate lithostratigraphically informal sandstone units recognised by previous authors (adapted from Bladon et al., 2015a).

134x124mm (300 x 300 DPI)

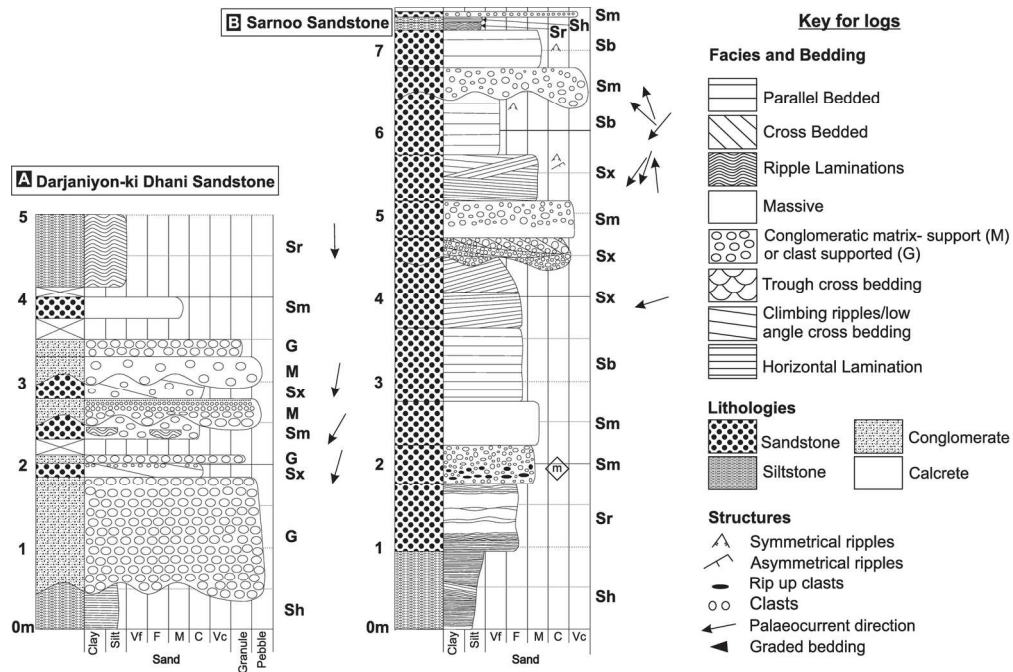
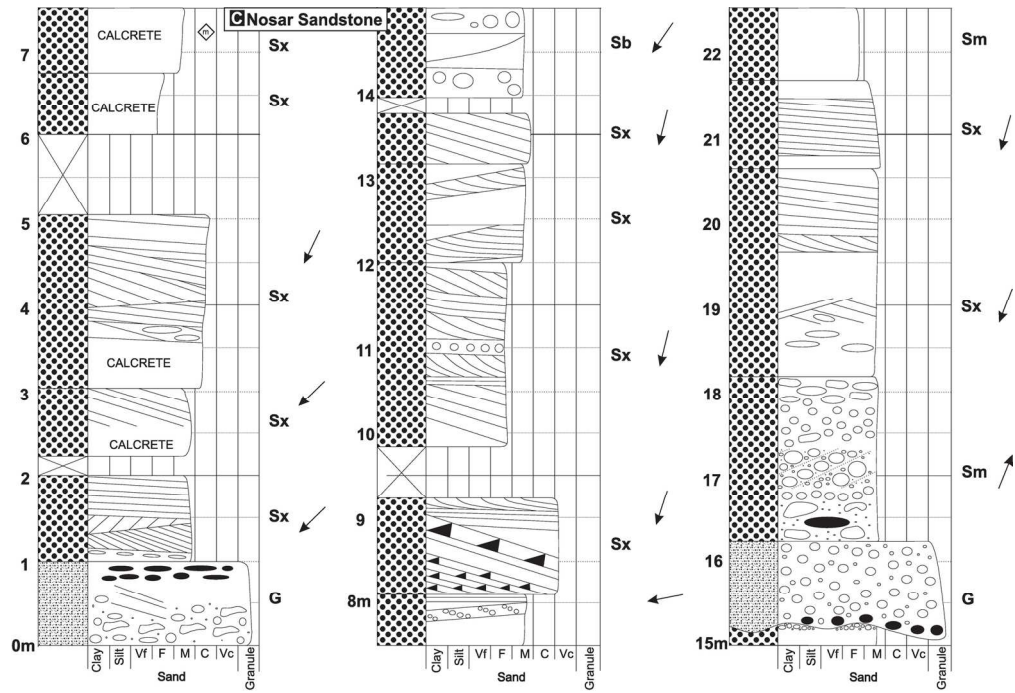


Figure 3: Simplified representative logs from the Ghaggar-Hakra Formation. Three logs displaying the typical facies from (A) the Darjaniyon-ki Dhani Sandstone, (B) the Sarnoo Sandstone and (C) the Nosar Sandstone. The facies codes stated on the logs are denoted in Table 1, the arrows represent the palaeoflow orientation and logs are in metres.

160x106mm (300 x 300 DPI)



160x109mm (300 x 300 DPI)

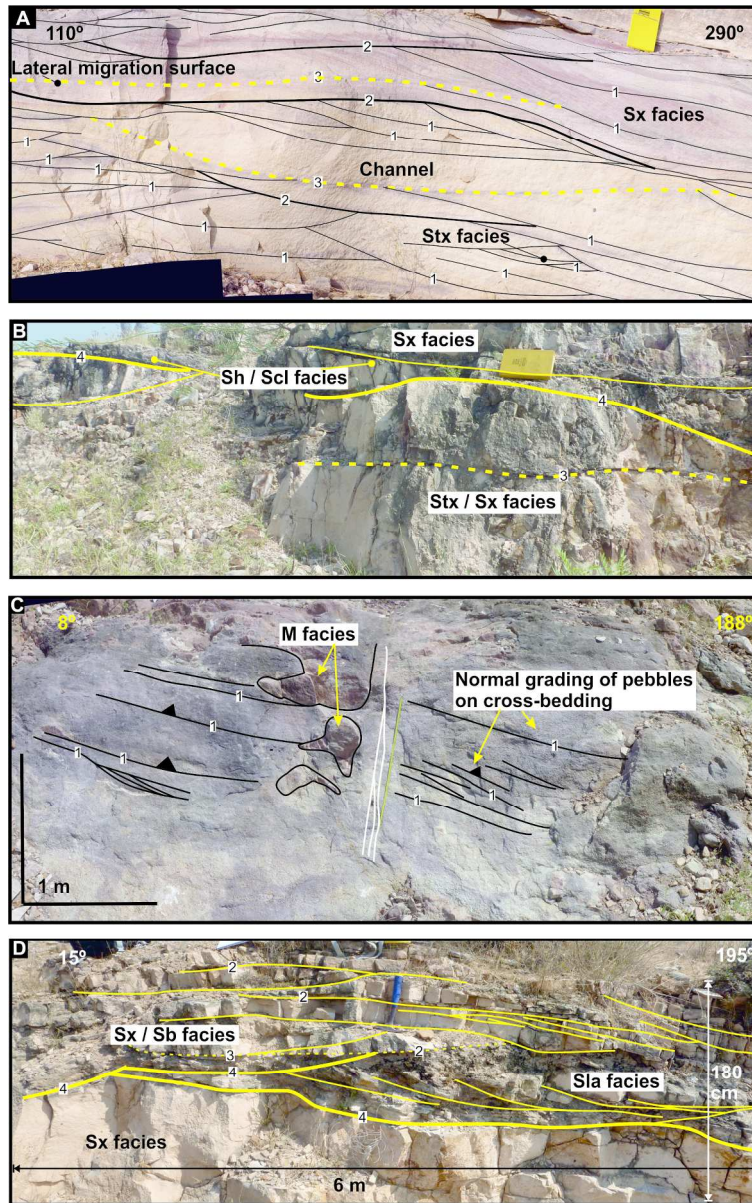
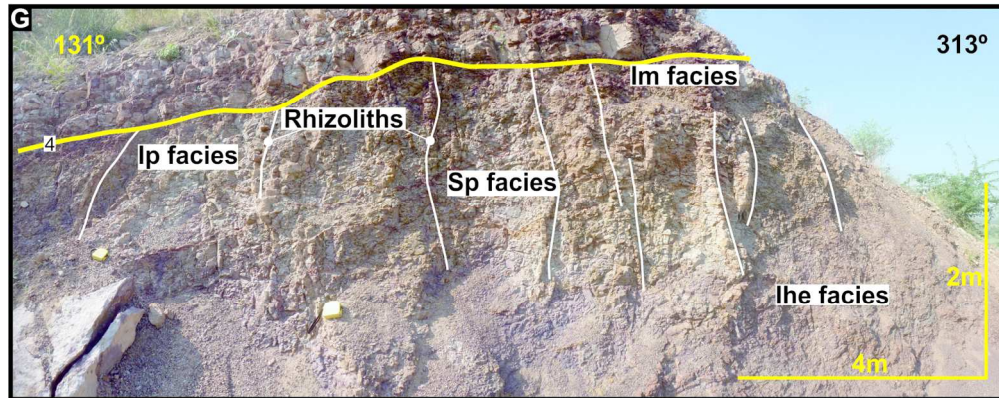
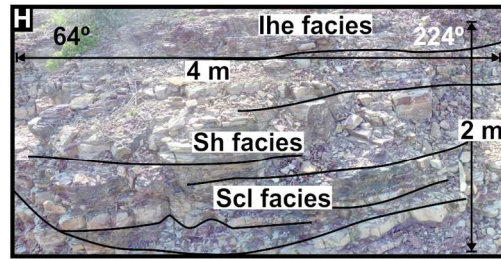
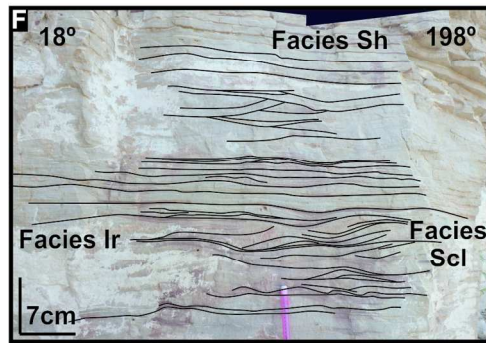
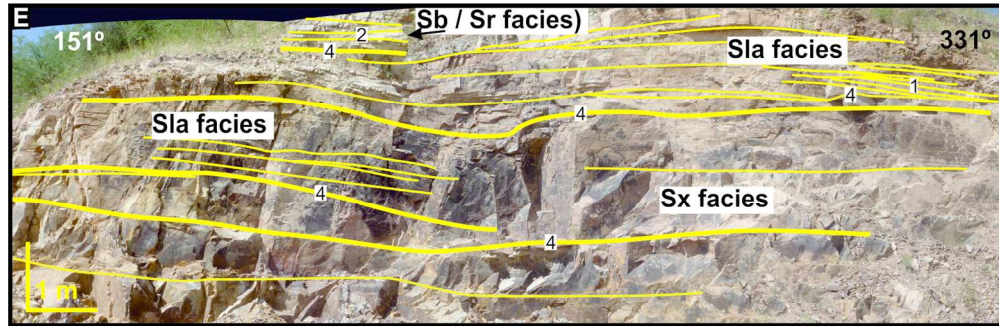


Figure 4: Interpreted photographs of the architectural elements (A) Channel element (Ch) displaying 1st – 3rd order bounding surfaces with the trough and planar cross-bedded sandstone facies; (B) Channel margin element (Cm) displaying the gradational change from the cross-bedded facies (Stx / Sx) into the cross / horizontal-lamination facies (Sh / Scl) overlain by an erosional surface and the planar cross-bedded facies; (C) Gravel bar element (Gb) displaying the conglomerate facies (M & G) with indistinct cross-bedding and upon some of the cross-beds there are graded clasts; (D) Chute channel element (Cc) this image depicts the channel element indicated by the planar cross-bedded facies (Sx), the Point bar element indicated by the low-angle cross-bedded facies (Sla) and the chute channel indicated by the thick, thin solid lines and the planar cross-bedded and planar horizontally bedded facies (Sx / Sb); (E) Point bar element (Pb) Low-angle cross-bedded facies (Sla) with 2nd and 4th order bounding surfaces laterally migrating into the channel element (Ch); (F) Sheet flow element (Sf), here the element displays the horizontal-laminated and cross-lamination facies (Sh / Scl) with various types of ripples; (G) Overbank element (Ob) indicated by the rhizoliths and the pedogenic facies (Sp / Ip / Ihe), and; (H) Pond element (Po) indicated by the horizontal-

laminated and cross-lamination facies (Sh / Scl).

155x247mm (300 x 300 DPI)



155x170mm (300 x 300 DPI)

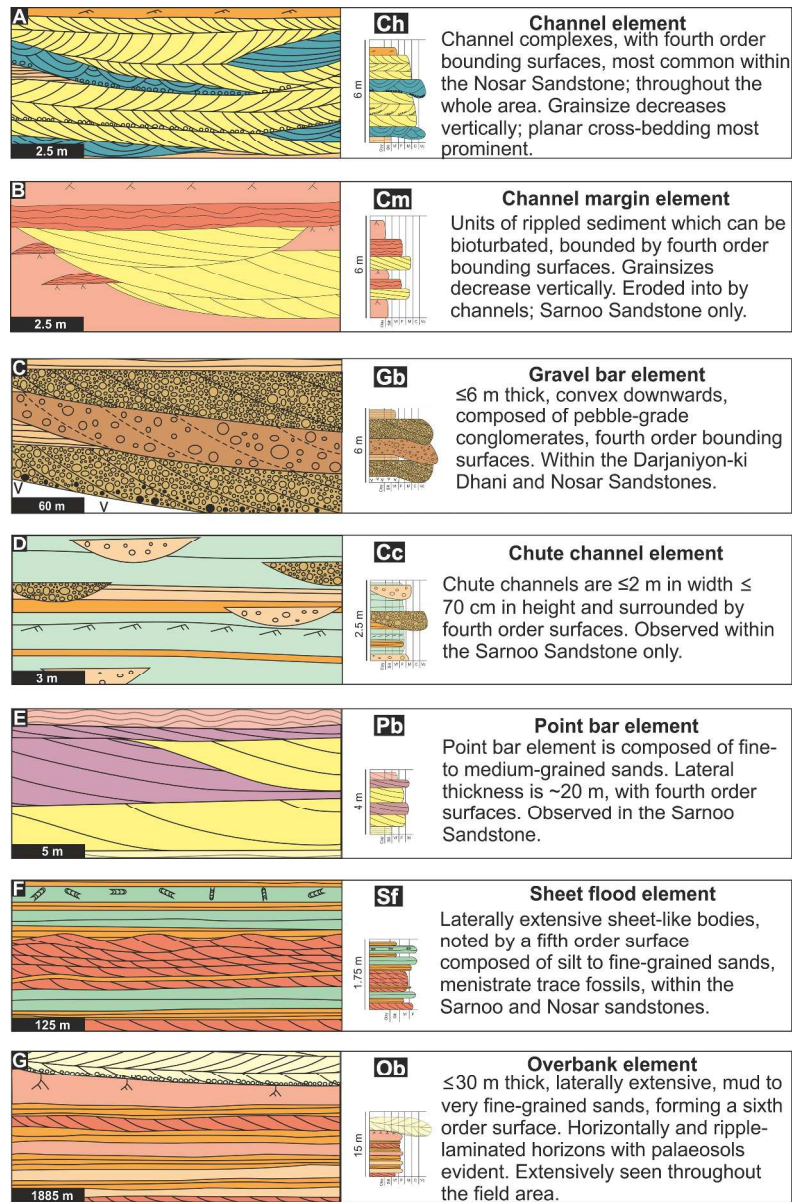
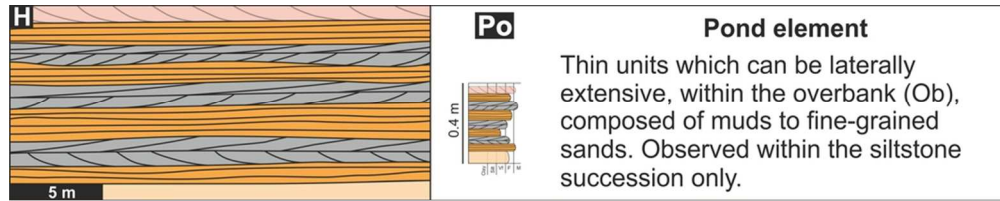


Figure 5: Two-dimensional sketches and logs that typify the architectural elements observed in the Ghaggar-Hakra Formation (A) Channel, Ch; (B) Channel margin, Cm; (C) Gravel bar, Gb; (D) Chute channel, Cc; (E) Point bar, Pb; (F) Sheet flow, Sf; (G) Overbank, Ob, and; (H) Pond, Po.

237x360mm (300 x 300 DPI)



- | | |
|--|--|
| Grain-supported conglomerate (G) | Trough cross-bedded sandstone (Stx) |
| Cross-bedded sandstone (Sx) | Parallel bedded sandstone (Sb) |
| Massive sandstone (Sm) | Low-angle cross-bedded sandstone (Sla) |
| Rippled sandstone (Sr) | Cross-laminated sandstone (Scl) |
| Horizontally-laminated sandstone / siltstone (Sh) | Matrix-supported conglomerate (M) |
| Pedogenic sandstone (Sp) / Pedogenic siltstone (Ip) / Haematitic pedogenic siltstone (Ihe) | Volcanics |
| Roots | Current ripples |
| | Trace fossils |

90x52mm (300 x 300 DPI)

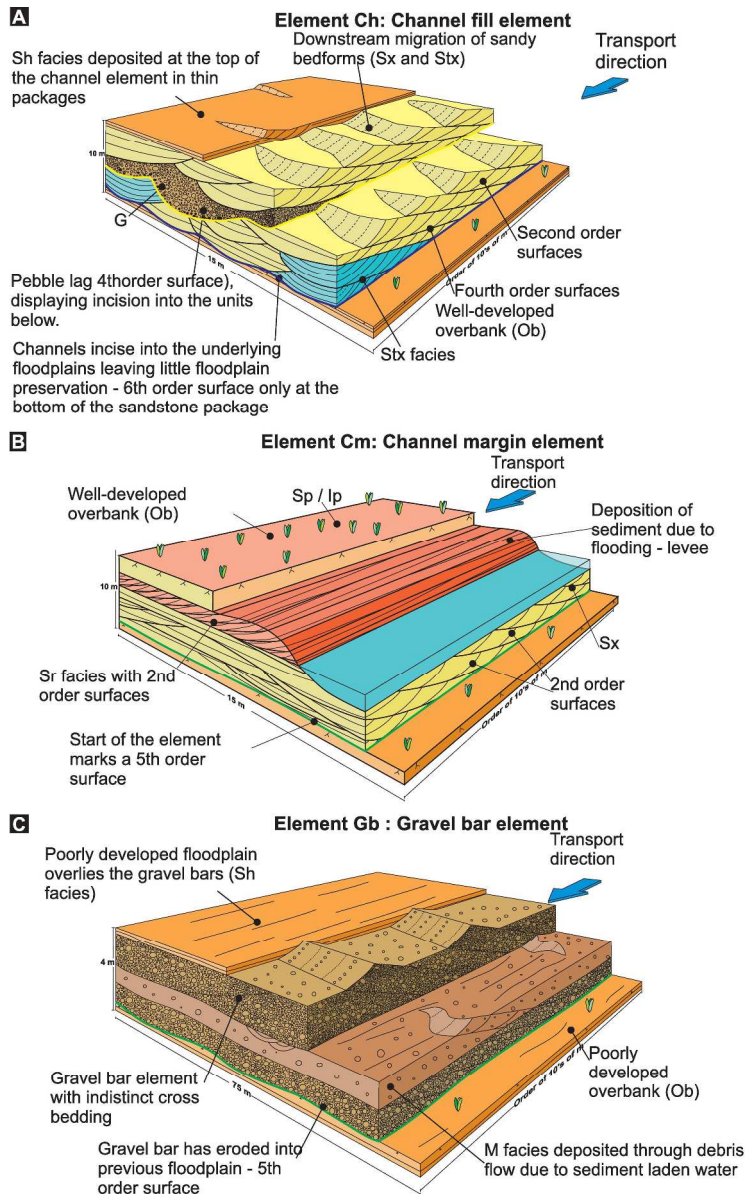
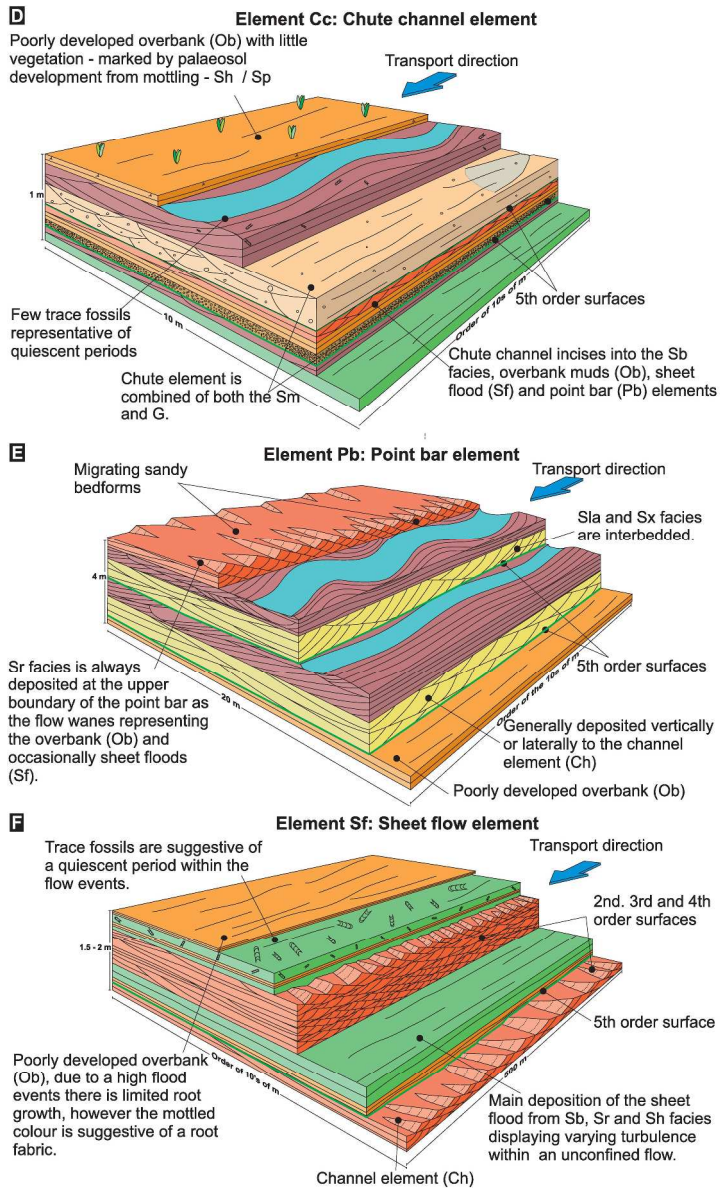
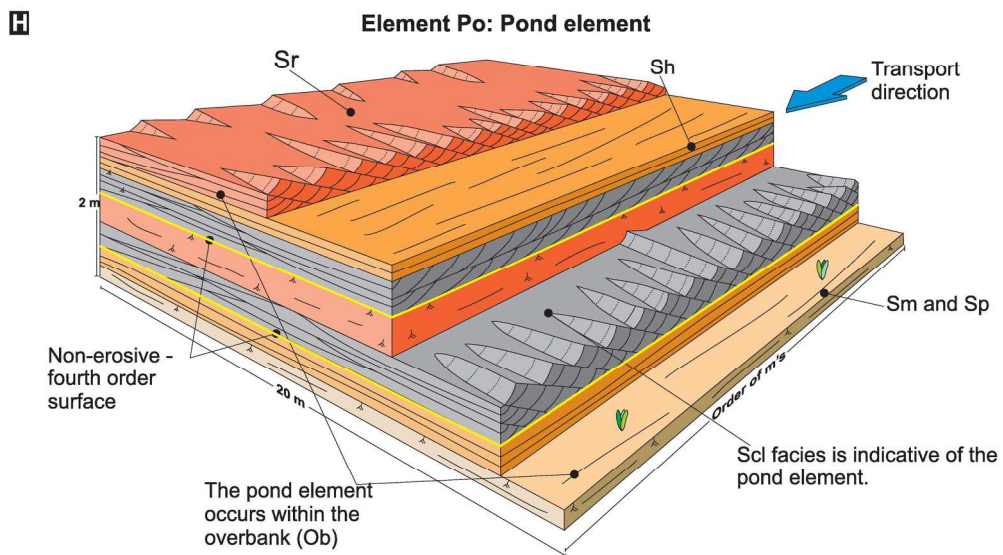
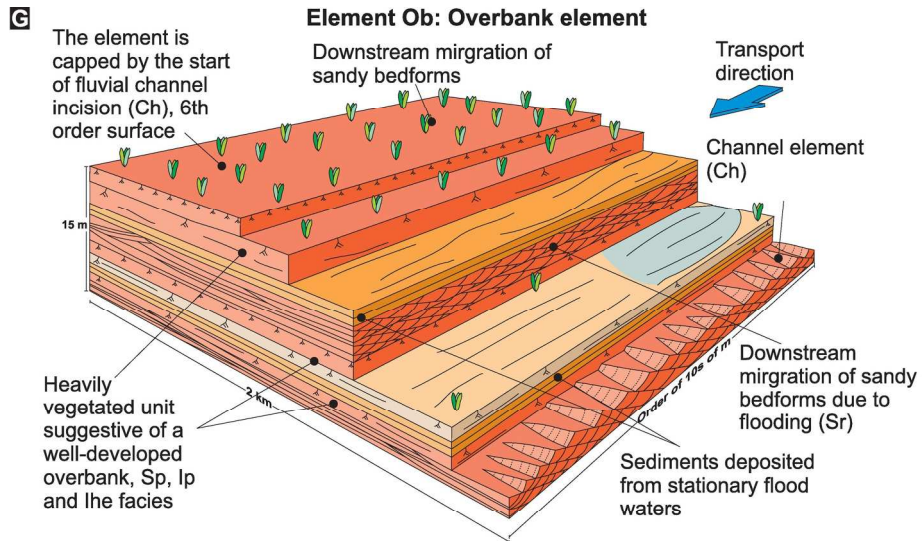


Figure 6: Three-dimensional facies models of the architectural elements; (A) The channel element (Ch) with an erosive lower base contains 1st to 3rd order surfaces internally; (B) The channel margin (Cm) element with an erosive lower base and 1st to 3rd order surfaces internally, the succession grades into the overbank; (C) The gravel bar (Gb) element with an erosive lower boundary and 1st to 2nd order surfaces within; (D) The chute channel (Cc) element with an erosive lower boundary and occasional first order boundaries within; (E) The point bar (Pb) element with an erosive 4th order boundary with 1st to 3rd order surfaces internally. This succession grades into the overbank; (F) The sheet flow (Sf) element starting with a lower 4th order bounding surface with 1st to 3rd order surfaces within. There are quiescent periods here evidenced by trace fossils; (G) The overbank (Ob) element with 1st, 2nd and 4th order surfaces within; (H) The pond (Po) element has a 4th order base and 1st to 2nd order surfaces internally.

244x390mm (300 x 300 DPI)



262x429mm (300 x 300 DPI)



187x207mm (300 x 300 DPI)

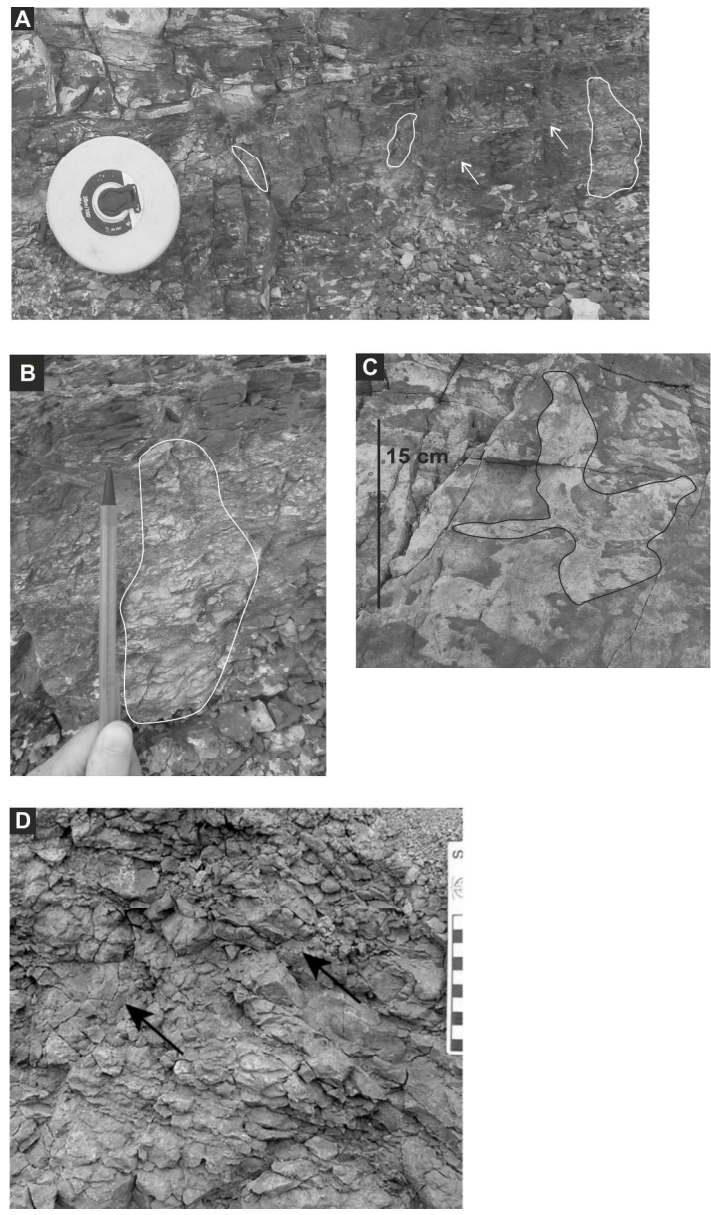


Figure 7: Rhizoliths within the floodplain (Ob) sediments (A) and (B) orange rhizoliths within the formation; (C) white reduction zones due to the organic material within the roots and rhizoliths, and; (D) the orange rhizoliths from Kraus and Hasiotis (2006), to allow for an easy comparison.

208x357mm (300 x 300 DPI)

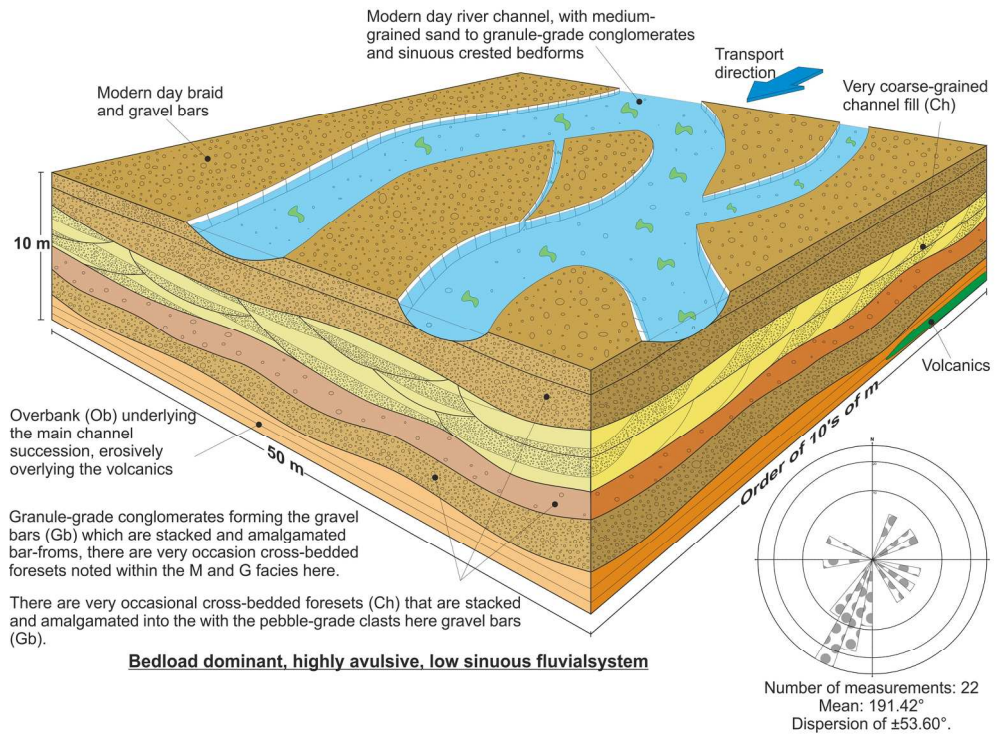


Figure 8: Facies model of the gravel bedload dominant low sinuosity fluvial system, the Darjaniyon-ki Dhani Sandstone, which contains the channel (Ch), gravel bar (Gb) and the overbank (Ob) architectural elements. There are 4th to 6th order bounding surfaces within. The sets and cosets within are inconsistent suggesting the gravel bars are transient, suggesting fluvial immaturity. The proportion of channels to floodplain is 90% to 10%, respectively.

179x134mm (300 x 300 DPI)

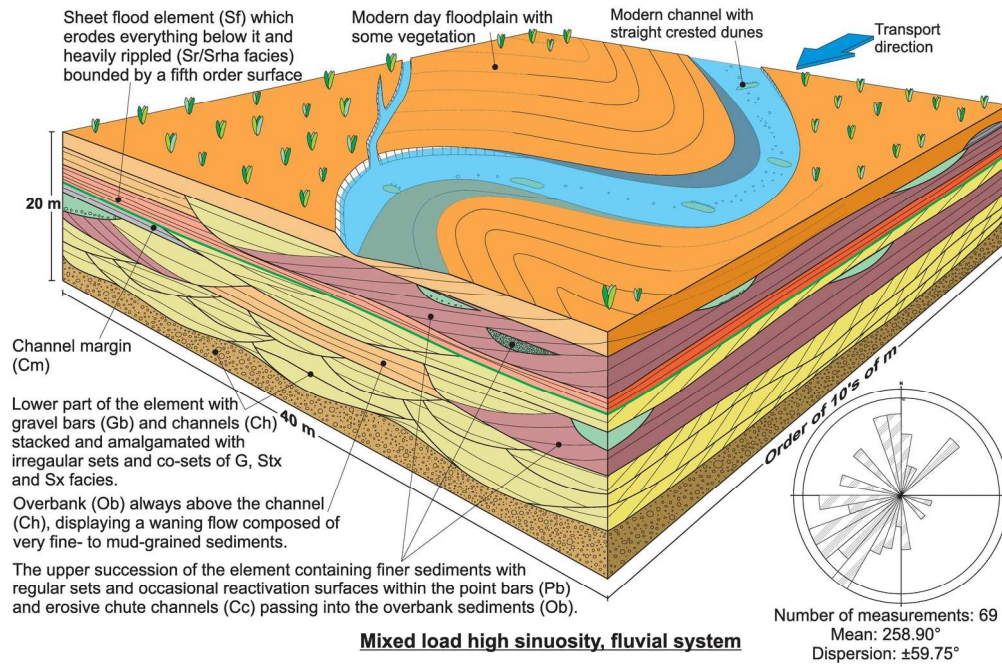


Figure 9: Facies model of the mixed load high sinuosity fluvial system, the Sarnoo Sandstone, as evidenced by the channels (Ch), channel margin (Cm), gravel bars (Gb), chute channels (Cc) sheet flows (Sf) and overbank (Ob) elements. The consistency of sets and cosets representing the migration of in-channel bedforms suggests discharge stability. The proportion of sand to mud increases from 80% sand and 20% mud to 60% sand and 40% mud vertically throughout the facies model.

169x114mm (300 x 300 DPI)

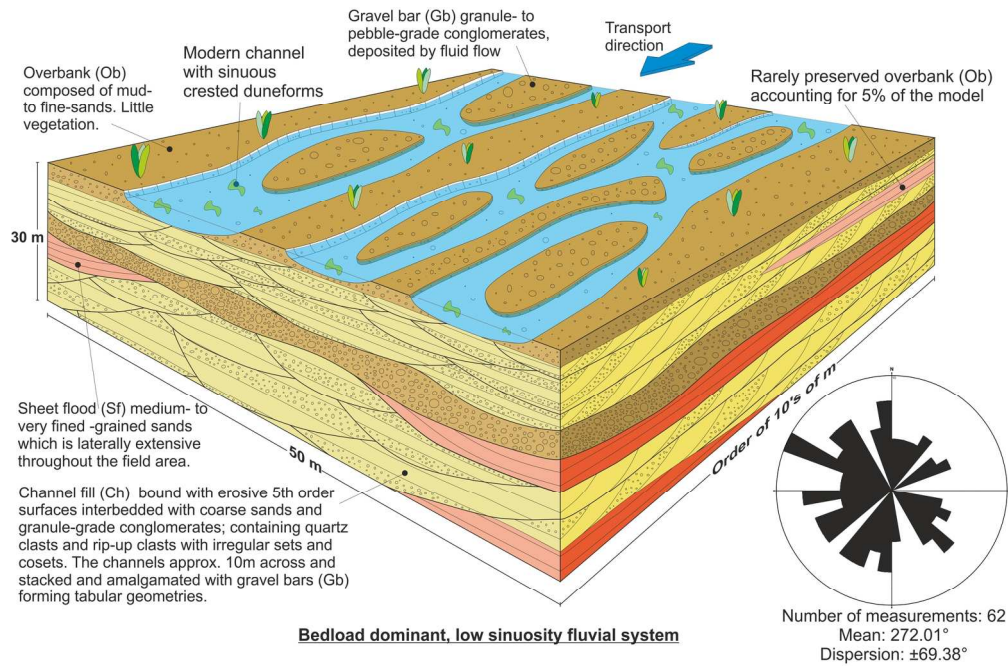
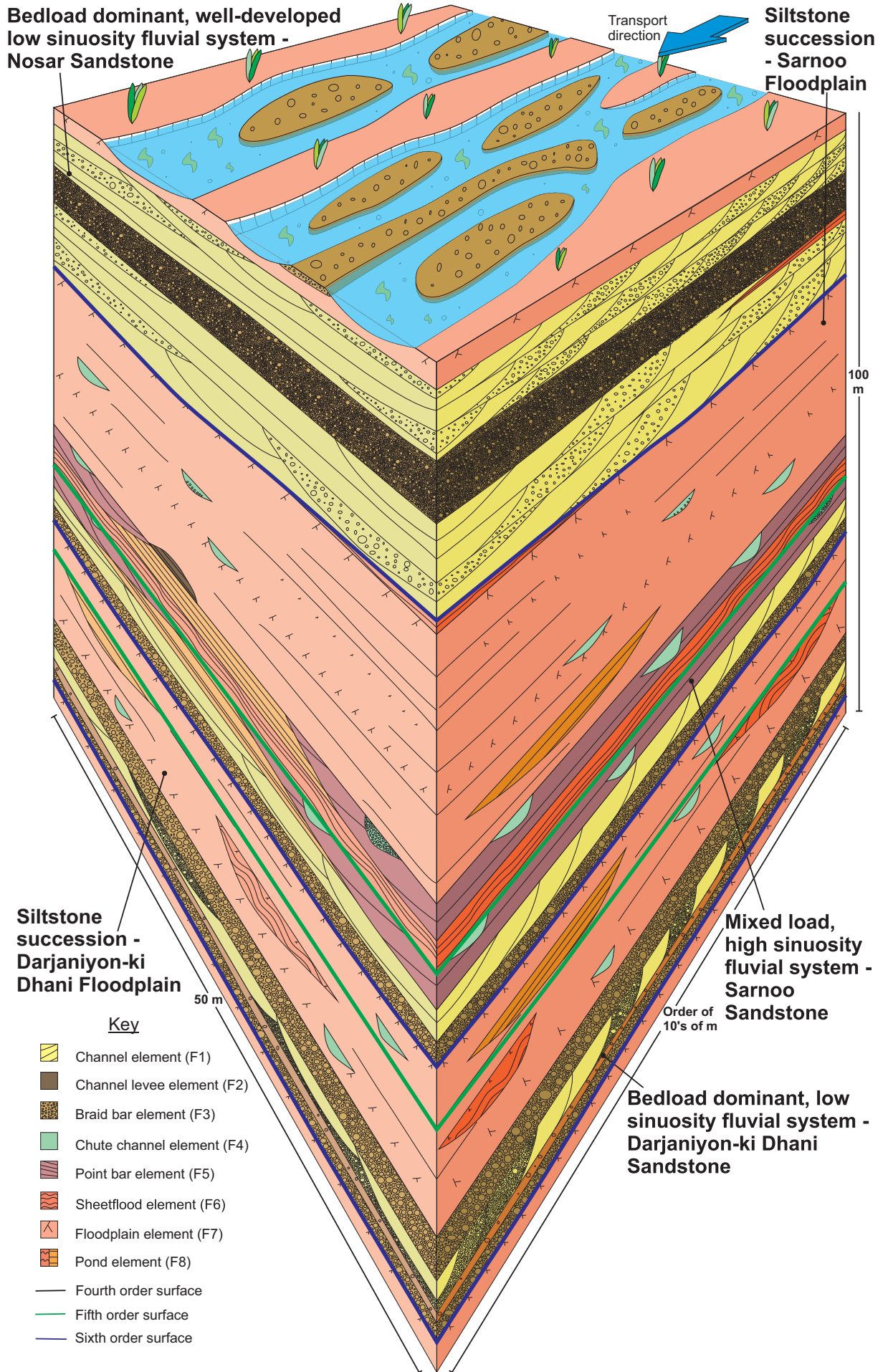


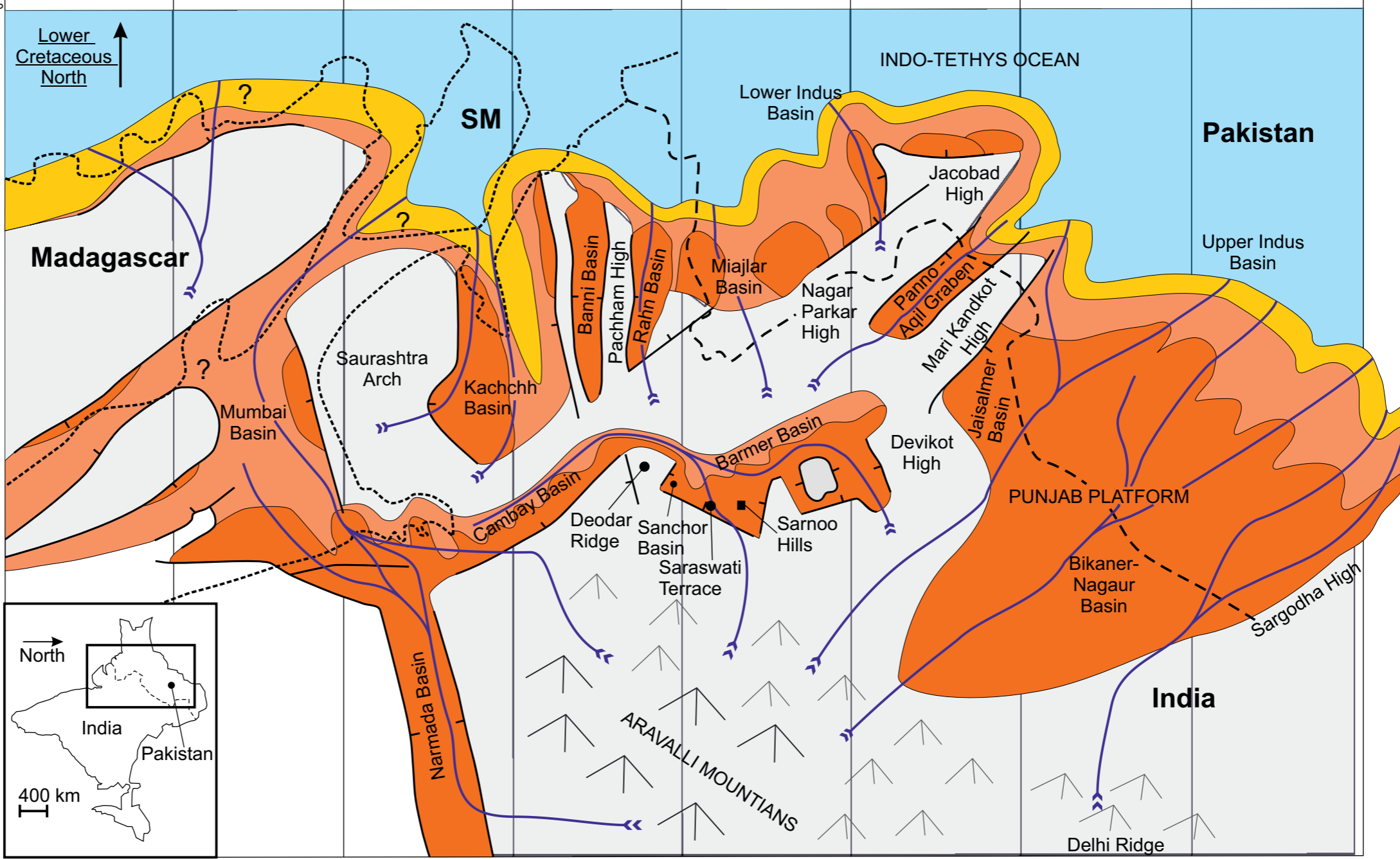
Figure 10: Facies model of a well-developed, bedload dominant, low sinuosity fluvial system, the Nosar Sandstone, displays channel (Ch), floodplain (Ob), gravel bars (Gb) and sheetflow (F6) elements. There are all six types of bounding surfaces within indicating erratic surfaces and multiple truncations. This suggests discharge irregularity and a high level of channel migration. The proportion of sand to mud is at 90:10.

169x115mm (300 x 300 DPI)

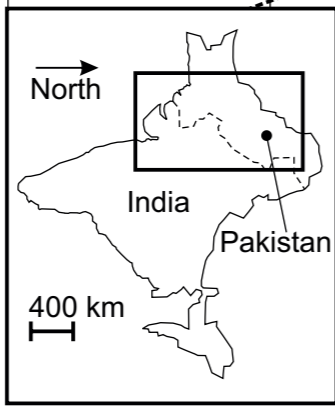


PDL: Present Day Location 16° 18° 20° 22° 24° 26° 28° 30° 32°
 LCL: Lower Cretaceous Location 26° 28° 30° 32° 34° 36° 38° 40° 42°

PDL: 66° LCL: -30°



- Key**
- |— Faults (with the tick on the downthrown side)
 - SM** Seychelles Microcontinent
 - - - India - Pakistan border
 - · · Land - ocean border
 - Boundary between different sedimentary environments
 - ? Limited or no data available
 - ⤴ Mountain (grey = smaller)
 - > Rivers; arrows indicate the direction of flow
 - High lands
 - Alluvial / proximal deposits
 - Fluvial systems
 - Shoreface / Deltaic
 - Open marine



PDL: 76° LCL: -40°